

FREE RADICAL INITIATED GRAFTING OF VINYL SILANE TO SATURATED
TRIGLYCERIDES

by

Oruç Nuri Köklükaya

B.S., Chemistry, Boğaziçi University, 2009

Submitted to the Institute for Graduate Studies in
Science and Engineering in partial fulfillment of
The requirements for the degree of
Master of Science

Graduate Program in Chemistry

Boğaziçi University

2013

*To My Family
And
My Dear Friends*

ACKNOWLEDGEMENTS

I would like to thank and present my sincere gratitude to my thesis supervisor Prof. Selim Küsefođlu for his guidance, support and belief in me. It will be always impossible for me to thank him enough for giving me the chance to work in this project and all the enlightenment and experience he granted me about both chemistry and life.

I would like to thank my committee members Prof. Duygu Semiz Avcı and Assoc. Prof. Sinan Ően for giving their valuable time in reviewing this thesis and for all their advices.

I would especially like to thank to Ekmel Helvacıođlu for his extensive help scientifically and many encouraging words. Without his help I would not be able to finish this thesis. My special thanks go to my laboratory partners for their friendship and help during my studies. I would also like to thank all my friends, colleagues and the members of the Chemistry Department and Hülya Metiner.

My final and deepest thanks are for my dear mother, father, brother, grandmother and my aunts for their loving hearts and all the years they spent in bringing me up so that I could show the endeavor to able to accomplish this project.

ABSTRACT

FREE RADICAL INITIATED GRAFTING OF VINYL SILANE TO SATURATED TRIGLYCERIDES

In this study silanized hydrogenated palm stearin was synthesized by reacting hydrogenated palm stearin with vinyltrimethoxysilane via free radical reaction. Dicumyl peroxide was used as initiator. The characterization of silanized-HPS was done by ^1H NMR and FT-IR spectroscopy. Homopolymer of silanized-HPS was synthesized by moisture curing. The silanized-HPS homopolymer was characterized by IR spectroscopy. The effect of the crosslink density upon moisture cure on the mechanical properties, thermal properties and swelling of silanized-HPS polymer was analyzed by surface hardness test, DSC (Differential Scanning Calorimetry), swelling test respectively. According to swelling test and surface hardness tests, silanized-HPS shows heterogeneous distribution of crosslinks in crosslinked areas. Hydrophobicity of silanized-HPS coated glass surface was studied by water contact angle measurements and the contact angles reach their maximum value of 107° .

ÖZET

VİNİLSİLANIN SERBEST RADİKAL BAŞLATICISIYLA DOYMUŞ TRİGLİSERİDE AŞILANMASI

Bu çalışmada, viniltrimetoksisilan serbest radikal başlatıcı ile hidrojene palm stearine aşılantmıştır. Dikünilperoksit reaksiyon başlatıcısı olarak kullanılmıştır. Silanlanmış hidrojene palm stearin ¹H NMR ve Fourier Transform Infrared Spektroskopisi (FTIR) kullanılarak karakterize edilmiştir. Silanlanmış hidrojene palm stearin su buharı ile kür etme yöntemi kullanılarak silanol gruplarından polimerleştirilmiştir. Sentezlenmiş homopolimer FTIR kullanılarak karakterize edilmiştir. Nemle kür etme yöntemiyle oluşan çapraz bağların silanlanmış hidrojene palm stearinin sırasıyla mekanik, ısı ve şişme özelliklerine olan etkisi yüzey sertliği, Diferansiyel Taramalı Kalorimetre (DSC) analizi, şişme testi ile incelenmiştir. Şişme testi ve yüzey sertliği testlerine göre, silanlanmış hidrojene palm stearin çapraz bağlanmış kısımlarında heterojen bir morfoloji göstermektedir. Silanlanmış hidrojene palm stearin kaplı cam yüzeyde suyun camdaki kontak açısı ölçülmüş ve maksimum değer olan 107° olarak ölçülmüştür.

TABLE OF CONTENTS

ACKNOWLEDGEMENTS	iv
ABSTRACT	v
ÖZET	vi
TABLE OF CONTENTS	vii
LIST OF FIGURES	ix
LIST OF TABLES	xi
LIST OF SYMBOLS	xii
LIST OF ACRONYMS/ABBREVIATIONS	xiii
1. INTRODUCTION	1
1.1. Renewable resources	1
1.2. Natural Oils and Fats	3
1.2.1. Chemical Structure and Properties of Oils and Fatty Acids	3
1.2.2. Chemistry of The Unsaturated Triglycerides.	6
1.3. Chemistry of Saturated Triglycerides.	9
1.3.1. Hydrogenation of Oils and Fats	12
1.4. Organo Functional Silanes	13
1.4.1. Uses of Organo Functional Silanes	15
1.4.1.1. Uses of Organo Functional Silanes.	15
1.4.1.2. Organofunctional Silanes as Surface Modifiers.	17
1.4.1.3. Organofunctional Silanes as Crosslinking Agents.	18
1.4.2. Vinyl Silanes	20
1.5. Polyethylene Crosslinking and Silane Grafting	21
2. OBJECTIVES.	24
3. EXPERIMENTAL	26
3.1. Materials and Apparatus	26
3.1.1. Materials	26
3.1.2. Analytical Instruments	26
3.2. Synthesis of Silanized Hydrogenated Palm Stearin.	28
3.3. Homopolymerization of Silanized Saturated Fat via Moisture Curing.	28

3.4. Surface Characterization of Silanized Saturated Fat Grafted Glass.	29
3.4.1. Contact Angle Measurement	29
3.5. Swelling Test.	29
4. RESULTS AND DISCUSSION	30
4.1. Characterization and Qualitative Analysis of Hydrogenated Palm Stearin	30
4.2. Synthesis and Characterization of Silanized-HPS.	33
4.3. Homopolymerization of Silanized-HPS	42
4.4. Thermal Properties	48
4.5. Swelling Test.	50
4.6. Adhesion and Homopolymerization of VTMS graft HPS on Glass Surface	51
4.7. Contact Angle Measurements	52
4.8. Surface Hardness Test	56
5. CONCLUSIONS	58
REFERENCES	59

LIST OF FIGURES

Figure 1.1.	The global consumption of petroleum in 2007 [2].	1
Figure 1.2.	The life cycle of polymers based on triglyceride oils [6].	2
Figure 1.3.	General triglyceride structure [5].	3
Figure 1.4.	Reactive centers of triglyceride.	6
Figure 1.5.	Chemical methods used to synthesize functionalized triglyceride [13].	8
Figure 1.6.	Chemical structure of tristearin.	9
Figure 1.7.	Hydrogenation of oils and possible products [32].	12
Figure 1.8.	General structure of organofunctional silane.	14
Figure 1.9.	Hydrolytic deposition and condensation of silanes [40].	16
Figure 1.10.	Silane bonding to inorganic surface [42].	18
Figure 1.11.	Moisture crosslinking of alkoxy silanes [43].	19
Figure 1.12.	The structure of vinyl silane.	20
Figure 1.13.	Grafting of vinyl trimethoxysilane initiation and propagation steps [54].	23
Figure 2.1.	Silanized HPS, coupling to inorganic surface and homopolymerization of the product.	25
Figure 4.1.	¹ H NMR spectrum of hydrogenated palm stearin.	31
Figure 4.2.	FTIR spectrum of hydrogenated palm stearin.	32
Figure 4.3.	Dicumyl peroxide decomposition.	33
Figure 4.4.	Vinyltrimethoxysilane grafting onto a hydrocarbon chain by the peroxide initiated radical method [59].	34
Figure 4.5.	1,5 Hydrogen-shift mechanism [56].	35
Figure 4.6.	¹ H NMR spectrum of vinyltrimethoxysilane.	36

Figure 4.7.	FTIR spectrum of vinyltrimethoxysilane.	37
Figure 4.8.	Structure of silanized-HPS.	38
Figure 4.9.	FTIR spectrum of vinyltrimethoxysilane grafted HPS.	40
Figure 4.10.	¹ H NMR spectrum of vinyltrimethoxysilane grafted HPS.	41
Figure 4.11.	Crosslinking reaction of VTMS γ HPS.	43
Figure 4.12.	FTIR spectrum of homopolymer VTMS grafted HPS.	45
Figure 4.13.	FTIR spectrum of DCM extracted VTMS γ HPS sample.	46
Figure 4.14.	FTIR spectrum of extract of VTMS γ HPS sample.	47
Figure 4.15.	DSC traces of silanized-HPS 5:1 and 3:1 after moisture cure.	49
Figure 4.16.	Swelling behavior of silanized-HPS with different mol ratio after moisture cure.	51
Figure 4.17.	Moisture curing process of organo functional alkoxy silanes.	52
Figure 4.18.	Surface tension vectors on a liquid droplet placed on a solid surface [13].	53
Figure 4.19.	The contact angle measurements of clean glass, silanized glass and VTMS-g- HPS solution casted glass.	54
Figure 4.20.	FT-IR spectrum of VTMS coated glass surface.	55
Figure 4.21.	Shore test results for HPS and silanized HPS.	57

LIST OF TABLES

Table 1.1. Some common fatty acids [6].	4
Table 1.2. Fatty acid composition of oils [6].	5
Table 1.3. Iodine values of some common fatty acids [6].	6
Table 1.4. Some common saturated fatty acids [20].	9
Table 1.5. Chemical composition of common animal fats [21].	11
Table 1.6. Some common organofunctional and siliconfunctional groups.	14
Table 1.7. Organofunctional silane usage as coupling agent [41].	17
Table 1.8. The use of silane as crosslinker [41].	20
Table 3.1. Vinyltrimethoxysilane properties.	26
Table 3.2. Hydrogenated palm stearin properties.	27
Table 4.1. The relationship between contact angle, degree of wetting and strength of interactions.	53

LIST OF SYMBOLS

% (w/w)	Mass-mass Percentage
CO ₂	Carbon dioxide
CDCl ₃	Deuterated chloroform
g	Gram
h	Hour
T _g	Glass Transition Temperature
V	Volume
γ	Grafted

LIST OF ACRONYMS/ABBREVIATIONS

Bp	Boiling Point
Cat.	Catalyst
DSC	Differential Scanning Calorimetry
DCP	Dicumyl peroxide
DCM	Dichloromethane
FTIR	Fourier Transform Infrared Spectroscopy
HPS	Hydrogenated Palm Stearin
IR	Infrared
MHz	Mega Hertz
Mp	Melting Point
MW	Molecular Weight
NMR	Nuclear Magnetic Resonance
PE	Polyethylene
ppm	Part per million
RT	Room Temperature
TMS	Tetramethylsilane
THF	Tetrahydrofuran
VTMS	Vinyltrimethoxysilane

1. INTRODUCTION

1.1. Renewable resources

Petroleum has been predominating raw material which was used in synthesis of polymeric materials [1]. World is widely dependent on petroleum for its properties and activities. Figure 1.1 shows the global consumption of petroleum in 2007. Almost every year, 90 % of the drilled oil is used and consumed by human beings as an energy source for transportation in vehicles and for electricity and heat generation. And rest is used as raw material for polymeric synthesis and in manufacturing of products such as solvents, plastics, lubricants, fibers, synthetic rubbers, detergents and others by chemical and petro chemical industries. Unfortunately, petroleum resources are limited [2].

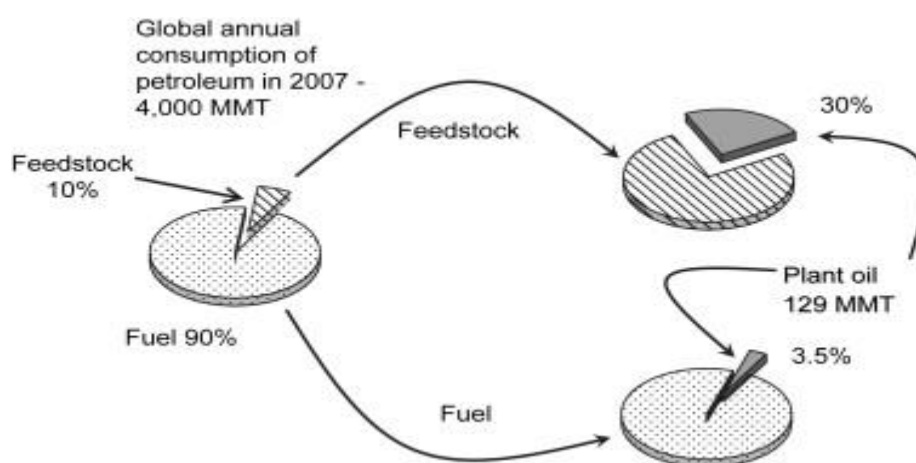


Figure 1.1. The global consumption of petroleum in 2007 [2].

Since petroleum is non-renewable and limited as this resource decreases, the price of petroleum increases accordingly [1]. Today one of the important subjects in environmental science is global warming. Burning petroleum releases carbon dioxide into the atmosphere which increases the average temperature of the earth [2].

Using renewable biomass as starting material as an alternative to petroleum based materials contributes to global sustainability, this will diminish the dependency on petroleum resources and reduce the danger of global warming [3, 4].

Hence, all of these reasons above force the chemical industry to search for new renewable resources. Due to their renewable nature, biodegradability, abundance, relatively low price and rich application areas plant oils and their derivatives are the most promising renewable raw material used by chemical industry [5]. Natural plant and animal oil sources are available worldwide and they are expected to be alternative chemical raw materials in the future. In addition to their applications in food industry, inexpensive triglyceride natural oils and fats have been used prevalently for coatings, inks, lubricants, plasticizers, resins and agrochemicals [3].

Furthermore, by applying diverse chemistry on plant oils, a large variety of monomers and polymers are obtained. In order to produce suitable polymerizable monomers high synthetic potential of plant oils is used [5]. Environmentally friendly natural oil based polymers have many advantages compared to petroleum based polymers. Figure 1.2 shows the cycle of triglyceride in polymerization [6].

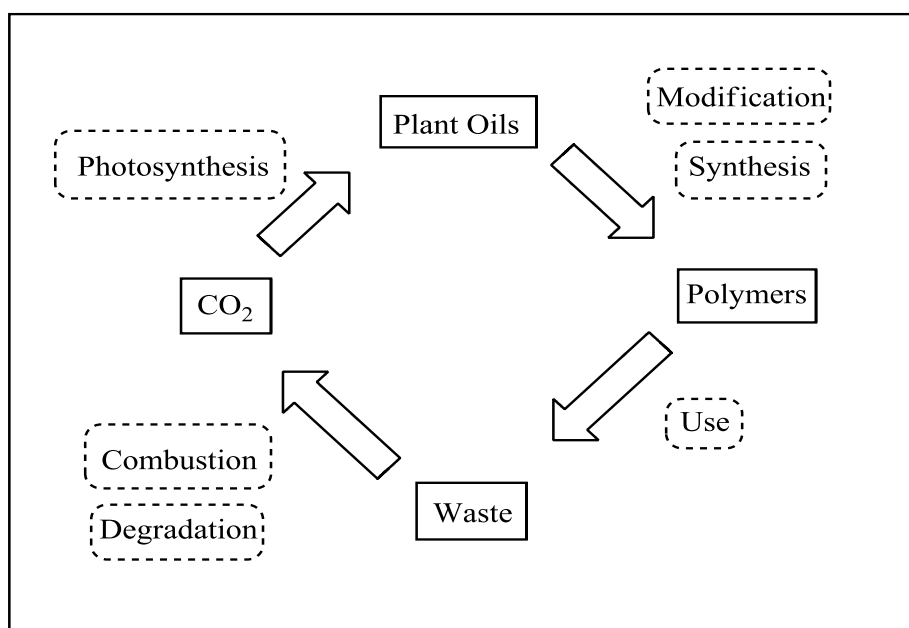


Figure 1.2. The life cycle of polymers based on triglyceride oils [6].

Moreover, load bearing, high-tech, durable polymers can also be synthesized by using natural plant oils [1].

1.2. Natural Oils and Fats

1.2.1. Chemical Structure and Properties of Oils and Fatty Acids

Due to their unique chemical and physical properties, fats and oils have been used throughout the years as fuels, foods, lubricants and starting material for other chemicals. Generally, oils and fats are derived from vegetable, animal and marine sources [7]. Plant oils and fats are the materials that are not water soluble. Oils are mainly composed of unsaturated triglycerides. Triglycerides are the esterification product of glycerol with three fatty acids. Figure 1.3 shows the structure of triglyceride molecule. Long alkyl chains are showed by R groups. Type of the plant from which the oil is obtained determines the chain length and functional groups on R [8].

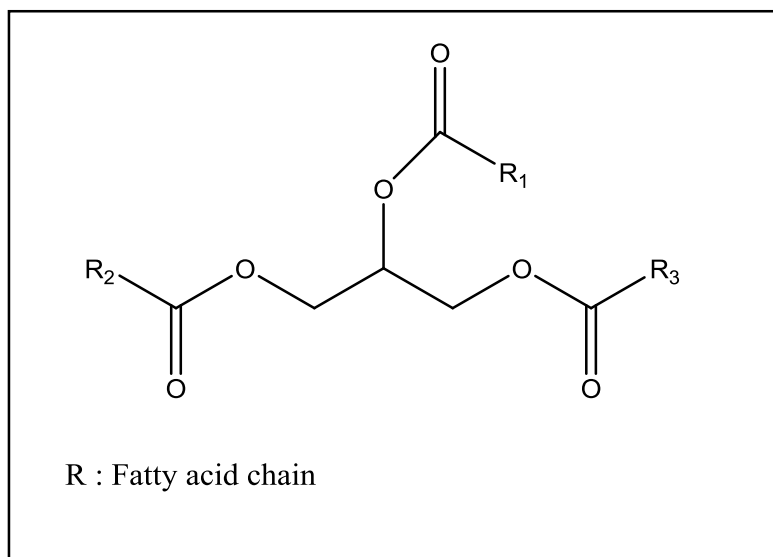
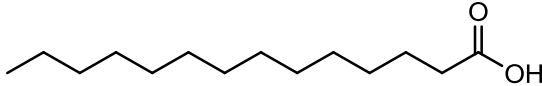
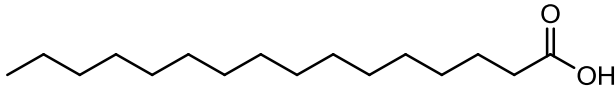
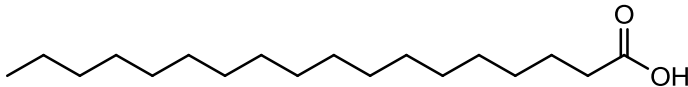
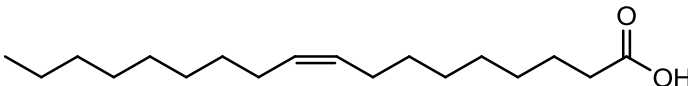
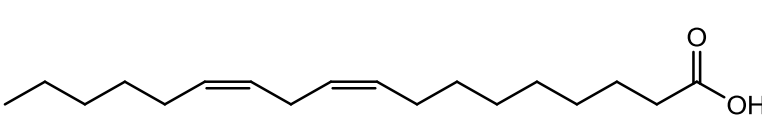
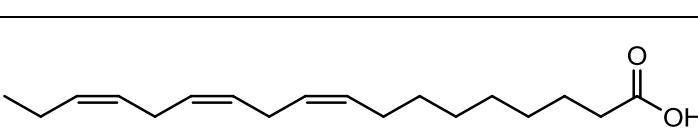


Figure 1.3. General triglyceride structure [5].

Fatty acids are usually aliphatic long chains with carboxylic acids. Aliphatic chain part of fatty acids usually have 14 – 22 carbon atoms [9].

The most common fatty acids in natural oil compositions are given in Table 1.1. Some of the acids are saturated and have no double bonds. Triglycerides that are formed from saturated acids are solid at room temperature and are called as fat. Fats are mostly obtained from animal source. On the other hand, some fatty acids are unsaturated and have double bond or bonds which exist as cis unconjugated isomer and are mostly obtained from plant sources [10, 11].

Table 1.1. Some common fatty acids [6].

Name	Formula	Structure
Myristic acid	$C_{14}H_{28}O_2$	
Palmitic acid	$C_{16}H_{32}O_2$	
Stearic acid	$C_{18}H_{36}O_2$	
Oleic acid	$C_{18}H_{34}O_2$	
Linoleic acid	$C_{18}H_{32}O_2$	
Linolenic acid	$C_{18}H_{30}O_2$	

Each oil has a unique distribution of fatty acid that determines the distribution of double bonds. Nowadays, by using genetic engineering, it is possible to control not only fatty acid distribution of plant but also the functional groups to triglyceride molecules [7]. Fatty acid composition of various oils is given at the Table 1.2.

Table 1.2. Fatty acid composition of oils [6].

Fatty acid	Costor oil (%)	Linseed oil (%)	Oiticica oil (%)	Palm oil (%)	Rapeseed oil (%)	Refined tall oil (%)	Soybean oil (%)	Sunflower oil (%)
Palmitic acid	1.5	5	6	39	4	4	12	6
Stearic acid	0.5	4	4	5	2	3	4	4
Oleic acid	5	22	8	45	56	46	24	42
Linoleic acid	4	17	8	9	26	35	53	47
Linolenic acid	0.5	52	-	-	10	12	7	1
Ricinoleic acid	87.5	-	-	-	-	-	-	-
Licanic acid	-	-	74	-	-	-	-	-
Other	-	-	-	2	2	-	-	-

Table 1.3. Iodine values of some common fatty acids [6].

Fatty acid	Number of carbon atoms	Number of double bonds	Iodine value of acid	Iodine value of triglyceride
Palmitoleic acid	16	1	99.8	95
Oleic acid	18	1	89.9	86
Linoleic acid	18	2	181.0	173.2
Linolenic acid	18	3	273.5	261.6
Ricinoleic acid	18	1	85.1	81.6
Licanic acid	18	3	261.0	258.6

1.2.2. Chemistry of The Unsaturated Triglycerides

The triglyceride molecule of oil has 4 active centers which can be used in chemical reactions. Figure 1.4 shows all active sites of triglyceride.

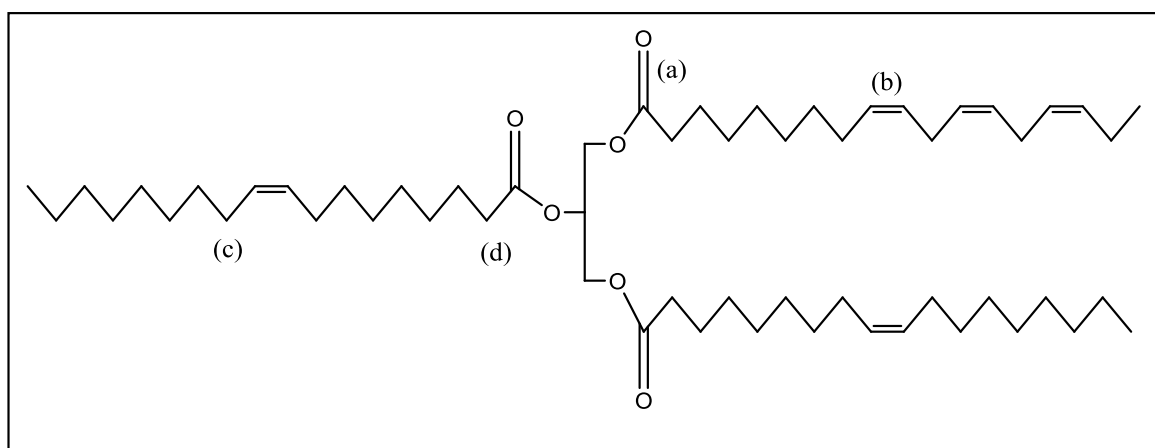


Figure 1.4. Reactive centers of triglyceride.

These groups are the carbonyl of ester group (a), double bonds (b), allylic carbons (c) and the α -methylene groups to carbonyl (d). These chemically active centers of triglycerides are used to functionalize the triglycerides by introducing polymerizable groups through synthetic techniques of organic chemistry [8].

Chemical modification of oils is an important way in producing useful products from renewable resources [12]. The reactions of triglycerides can be basically classified in three groups: the reactions on the carbonyl of ester group, the reactions on the double bond of aliphatic chain and the reactions on the hydrocarbon chain [13]. Some common monomer syntheses through chemical modification of triglycerides that have been introduced by our research group are illustrated in Figure 1.5.

The double bond on a fatty acid is the most reactive part of triglyceride. Some of the important reactions which use unsaturation of oil are hydrogenation, epoxidation, oxidative scission, carboxylation, Diels-Alder, ene reaction, olefin metathesis, cross metathesis and dimerization reactions [7]. The double bond functionalization of triglyceride facilitates the conversion of unsaturation to epoxy (b) and hydroxyl functionalities (c). Maleates can also be attached to triglyceride by using the double bonds (a) [14]. Further modification of epoxy and hydroxyl functionalized triglyceride is also possible with acrylic acid to attach vinyl functionalities (d). The reaction of maleic anhydride and hydroxyl containing triglyceride results in maleate half ester attached on triglyceride back bone [15, 16]. Moreover, acrylate can also be used to functionalize the triglyceride by one step addition of bromine and acrylate groups to a double bond in the presence of acrylic acid and N-bromosuccinimide [17].

The conversion of triglyceride molecule to monoglyceride through glycerolysis reaction or amidation reaction is one of the methods to synthesize polymerizable monomer from triglyceride (h), (i) [18]. The conversion of triglyceride molecules to monoglycerides and functionalization of double bond can be combined. For instance, either glycerolysis of an unsaturated triglyceride can be followed by hydroxylation or hydroxyl functionalized triglyceride can be glycerolized (j),(k) [8].

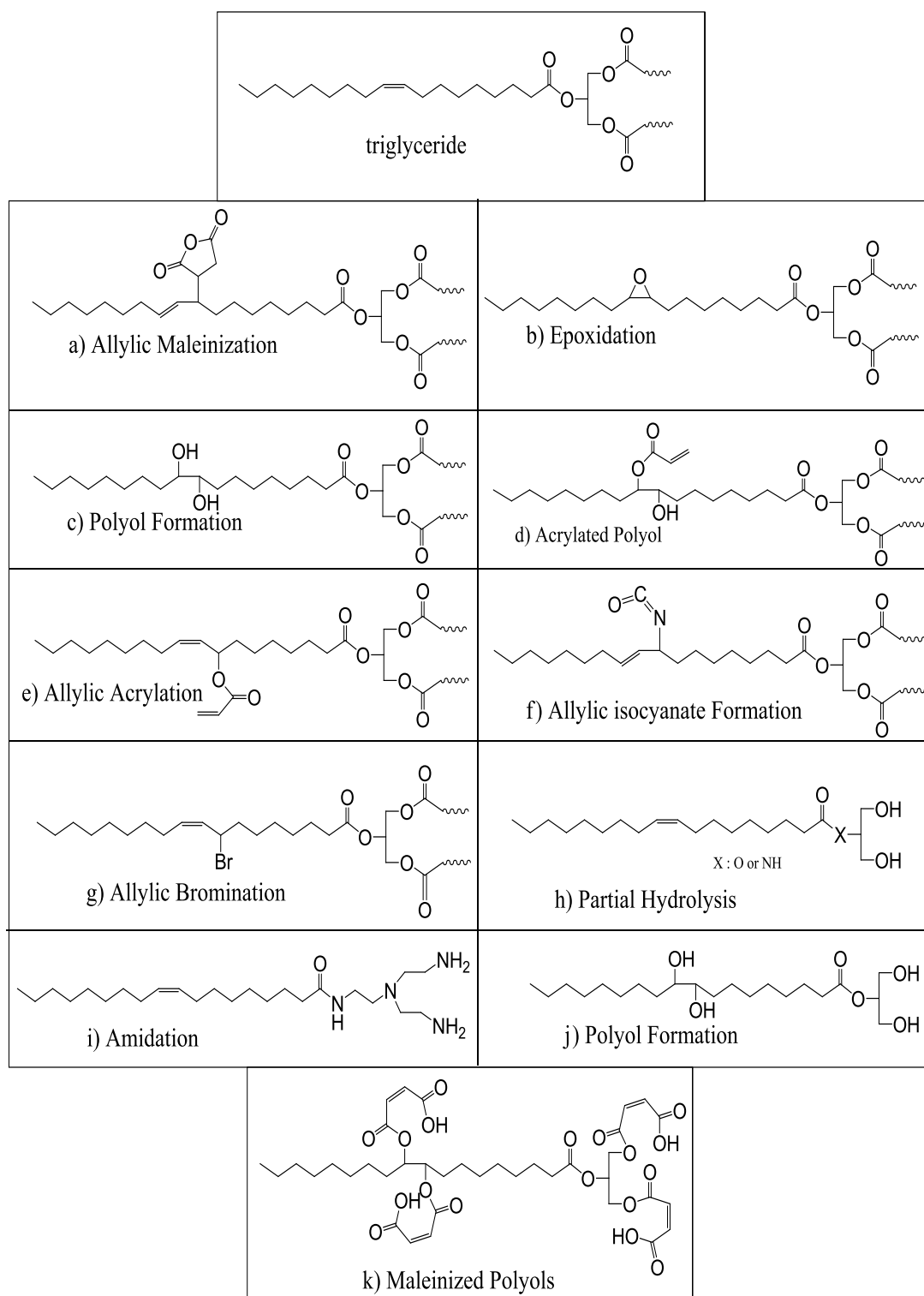


Figure 1.5. Chemical methods used to synthesize functionalized triglyceride [13].

1.3. Chemistry of Saturated Triglycerides

Saturated fats are composed of saturated fatty acids which contain no double bonds [19]. Tristearin chemical structure, three units of saturated stearic acid is shown in Figure 1.6. Some common saturated fatty acids and containing products are given in Table 1.4.

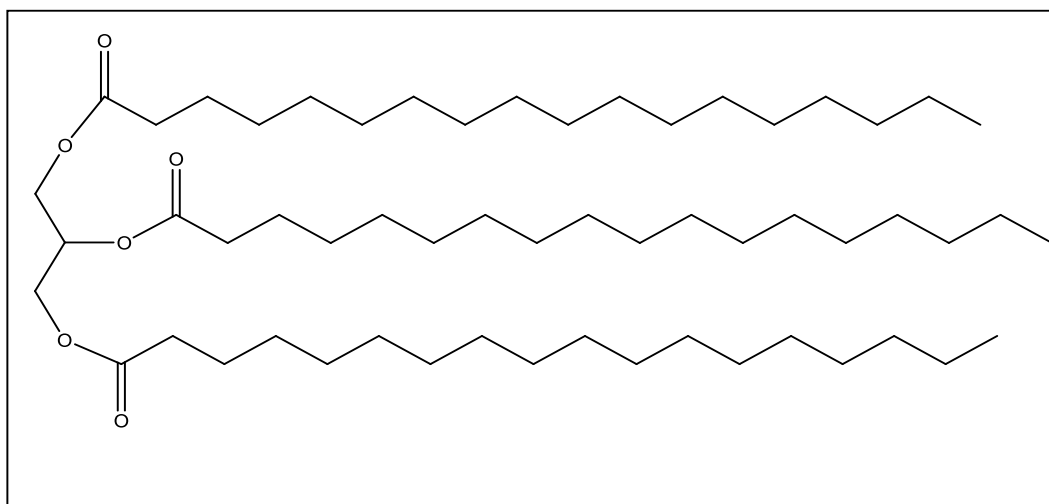


Figure 1.6. Chemical structure of tristearin.

Table 1.4. Some common saturated fatty acids [20].

Name of fatty acid	Number of carbon atoms	Source
Butyric acid	4	Butter
Lauric acid	12	Coconut oil, palm kernel oil, breast milk
Myristic acid	14	Cow's milk and dairy products, Lard
Palmitic acid	16	Palm oil, meat and lard
Stearic acid	18	Meat, cocoa butter and lard

Chain lengths and saturation level of these fatty acids influence the reactions and reactivity [21].

Iodine value is used to determine the amount of unsaturation in fatty acids and triglycerides. Iodine compounds react with the carbon carbon double bond. The mass of iodine in grams that is consumed by 100 grams of a chemical substance with unsaturation gives the iodine value of fatty acid or its triglyceride [20].

Saturated and unsaturated fatty acid proportions of all fats show wide variety. For instance, lard (pork fat) and tallow (beef fat) are the principal sources of the saturated and mono unsaturated C_{16} and C_{18} fatty acids such as palmitic, stearic and oleic acids [1]. Chemical composition of animal fats is given in Table 1.5. There are no natural sources that provide completely saturated triglycerides. Even the so called “saturated fats” contain enough unsaturation to give iodine values around 30.

Tallow and lard are mainly used as cooking fat or shortening and also used in biofuel and soap manufacturing. Similarly to animal fat source, plant originated oils and fats can have saturated fatty acid structure. Such as coconut oil, palm kernel oil and cocoa oil. Coconut oil and palm kernel oil (lauric oils) are composed of fatty acid with short or medium chain length, mainly 12 and 14 carbon atoms. These are especially suitable for further processing to surfactants for cosmetics, washing detergents and cleansing agents [19, 22].

Fat is non-uniformly stored and distributed in different parts of the animal and the quality depends basically on the nutrition of the animal. Fat which is located at the surface of the meat can be trimmed. The process called rendering is converting any animal product in to more useful and stable materials. The rendering process separates and isolates the fat from any other tissue. Edible fats, consumed as human food such as tallow and lard are rendered from muscle and bone tissue [21].

Table 1.5. Chemical composition of common animal fats [21].

Carbon Chain Length and Unsaturation	Beef Tallow	Pork Lard	Poultry Fat
¹² C Lauric	-	-	0.5
¹⁴ C Myristic	3.0	1.5	1.5
¹⁵ C Pentadecanoic	0.5	-	-
¹⁶ C Palmitic	24.0	27.0	22.5
¹⁶ C 1=Palmitoleic	2.5	3.0	8.5
¹⁷ C Margarinic	1.5	0.5	-
¹⁸ C Stearic	20.0	13.5	5.5
¹⁸ C 1=Oleic	43.0	43.5	40.0
¹⁸ C 2=Linoleic	4.0	10.5	19.0
¹⁸ C 3=Linolenic	0.3	0.5	1.0
²⁰ C Arachidic	0.5	-	-
Iodine Value	48	65	90
Saponification	200	200	196
Titer C-fatty acid basis	43	36	32

In many medical studies, it has been found that consuming saturated fatty acids increase blood cholesterol levels which increase the risk of atherosclerosis. On the other hand mono and poly unsaturated fatty acids decrease blood cholesterol levels. Thus a majority of people has begun to consume vegetable oils instead of animal fats in their diets [23]. In the latter half of the 20th century the diet preference of the western world showed a major shift from saturated to unsaturated oils. The meat industry responded by finding methods that can remove saturated fats from meat. Various techniques can be used to separate fat tissue from meat. For example, mechanical removal of some fat from meat by a crusher or cutting tool has been accomplished. Heat, light and centrifuge have been used in thermal rendering. Fat can also be separated from meat by solvent extraction. Supercritical carbon dioxide is used as an alternative extraction medium. Strong chemical

reagents such as acids are also treated for removal of fat [24-31]. If these processes come into widespread commercial use, there will be a large supply of saturated fat. A new and high tech use of this fat would be commercially successful as it would convert a waste product to a useful raw material. Due to the lack of chemical functionality, this raw material is used in low tech soap and candle production. Vinyl silane grafting to saturated fats will provide high tech application areas for saturated fats.

1.3.1. Hydrogenation of Oils and Fats

Hydrogenation is the addition of hydrogen atom pairs to a molecule that has unsaturations, usually an alkene. Three components are required for hydrogenation; the unsaturated substrate, hydrogen source and a catalyst. In Figure 1.7, hydrogenation of oils and possible products are given.

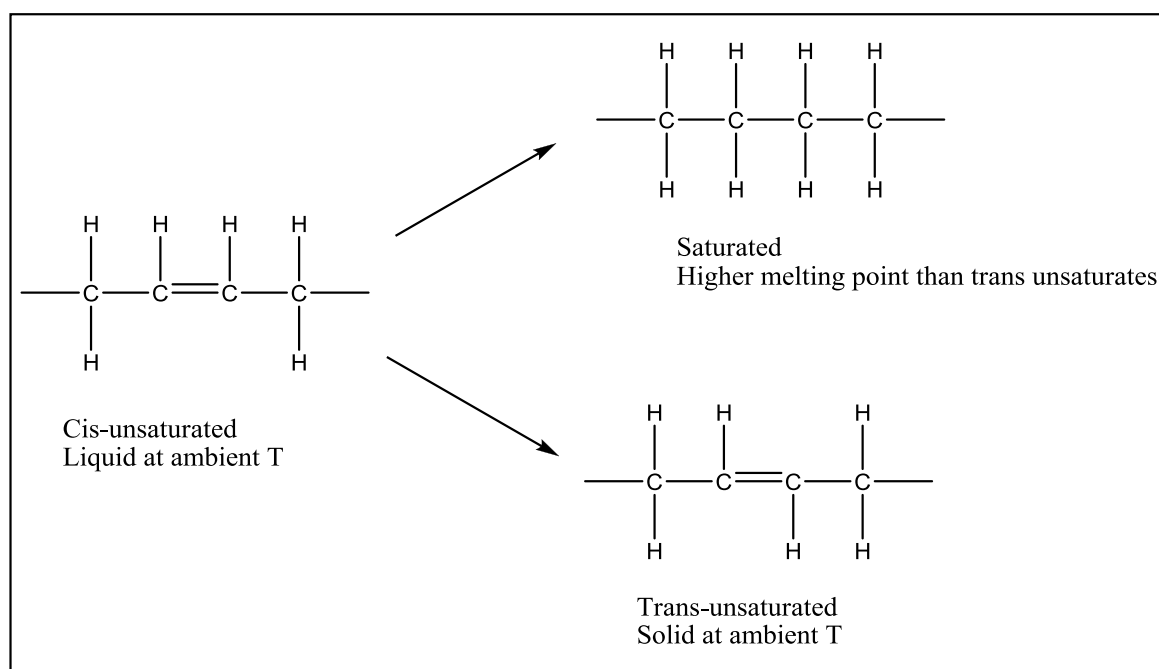


Figure 1.7. Hydrogenation of oils and possible products [32].

The hydrogenation of vegetable oils and fats is an important reaction in the process of modification of edible fats and oils. Hydrogenation is used to modify the oxidative and thermal stability of fats and oils. Vegetable oils can be converted from liquids to solids or semi-solids by hydrogenation reaction. Margarines and shortenings are obtained by this

way. Reducing the unsaturation content of oil to a minimum level improves the stability of oil against oxidative rancidity [33]. Unsaturation level of oil and fat is expressed with iodine value. Thus, with hydrogenation oil is saturated and iodine value is reduced to desired value [23]. Most of natural oils present C=C double bonds in cis geometry. During the hydrogenation, in addition to saturation of the double bonds, reactions of isomerization also take place. Conversion from cis to trans isomer will cause an increase in trans isomer content in the oil or the fat. Since trans isomers are shaped in a more linear form allow oils and fats to have better packing compare to cis isomers. As a result melting point of oils increase [34]. In spite of the commercial success of margarines, the presence of saturated and trans-unsaturated fatty acids in margarines continue to raise serious arguments on the health risks involved in their consumption.

1.4. Organo Functional Silanes

Silanes are coupling agents that have the ability to form a covalent bond between organic and inorganic materials. Organofunctional silanes are bi-functional molecules which have an organic reactive end and an inorganic end. Silanes are compounds that can react with wide range of organic and inorganic materials. They act as coupling agents, crosslinking agents and surface modifiers in many applications of adhesives, coatings and composite polymers. In Figure 1.8 general formula for an organosilane coupling agent is given and in Table 1.6 some examples for organofunctional and hydrolysable groups are shown [35].

There are reactions at the organic and inorganic end of the silane. The organofunctional part of silane is designed to react with an organic polymer and can be any of the followings, amino, epoxy, methacryl, vinyl, mercapto, urea and isocyanate. The organic group is chosen depending on the polymer. The organic compatibility between silane and organic polymer is achieved through reaction of organo silane with polymer or co-polymerization into the resin system. The covalent bond formation will provide strong connection between silane and polymer [8, 36].

Silicon functional group is a hydrolyzable group. Inorganic reactive end of alkoxy silane can be alkoxy, acyloxy, halogen and amine. The X groups hydrolyze to form silanols and can undergo condensation reactions with other silanols or hydroxyl groups on metal or glass surfaces and liberates water. Hydrolysis followed by condensation forms strong covalent bonds [35, 36]. The chemical reactions are shown in Figure 1.9.

1.4.1. Uses of Organo Functional Silanes

General application areas for organofunctional silanes are adhesion promoter/coupling agent, surface modifiers and crosslinking agents [37].

1.4.1.1. Uses of Organo Functional Silanes. The use of organofunctional silanes as adhesion promoters between inorganic materials and organic polymers has been proven in an ever increasing number of applications. Organofunctional silanes are able to act as excellent compatibilizers because of their dual character. They increase the interfacial adhesion between inorganic substrate and organic polymer and mechanical properties of composite material can be improved [8, 36].

The organofunctional group of silane links with polymer resin through covalent reaction or physical interaction. This group must be selected to provide maximum compatibility with polymer. The inorganic functional end of silane reacts with filler or substrate in two-step reaction. First step is hydrolysis. The alkoxy groups of the silane are hydrolyzed to the silanol and an alcohol is eliminated in this step. Second step is condensation. Condensation results in oligomer formation of silane and a bond formation between organic and inorganic materials. Silanol hydroxyls form hydrogen bond with hydroxyl groups of substrate and upon release of water covalent bond formation occurs. In Figure 1.9 hydrolytic deposition and condensation of silanes are given [35, 36, 38, 39]. In Table 1.7, silane area of usage as coupling agent is shown.

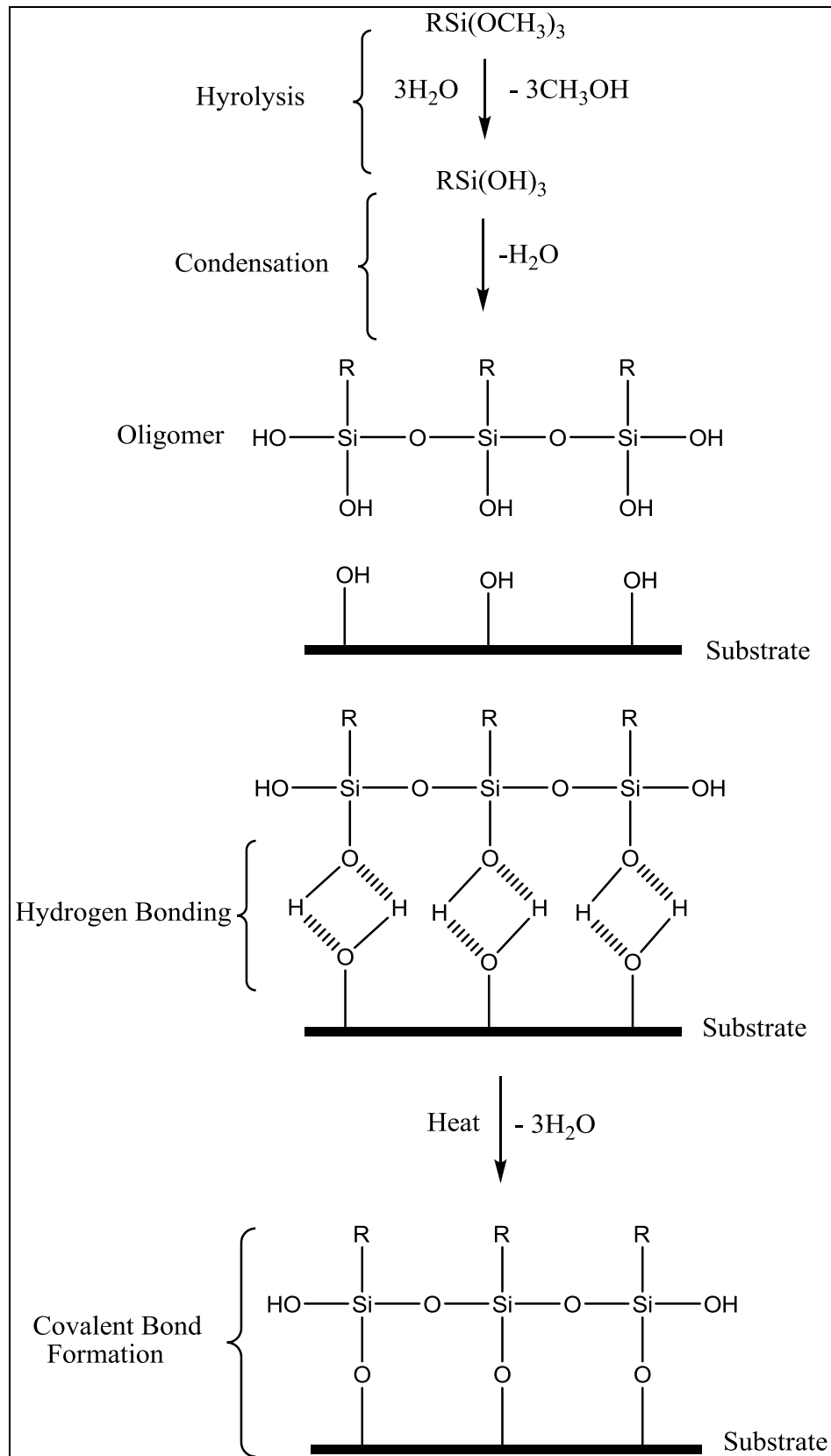
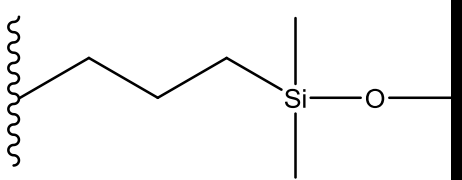


Figure 1.9. Hydrolytic deposition and condensation of silanes [40].

Table 1.7. Organofunctional silane usage as coupling agent [41].

 <p>As coupling agent for use in</p>	
Adhesives Sealants	Wet adhesion, Adhesion to difficult substrate
Glass Fiber	Resiliency of insulation batts, wet strength and electrical properties
Filler Treatment	Filler dispersion in thermoset and thermoplastic resins
Textiles	Water repellency , Dye receptivity, Hand feeling

1.4.1.2. Organofunctional Silanes as Surface Modifiers. Silanes improve the hydrophobicity of surface that they are applied on. The water absorption of the surface of the inorganic substrate is reduced by silanes usage. The use of silanes as compatibilizers improves certain characteristics of filler and polymer matrices. For instance, silanes reduce viscosity, improve processing, increase out put, reduce agglomeration, reduce total cost and allow higher filler loading. Application of silanes on inorganic substrate such as aluminum, concrete or glass, makes these substrate water repellent and more resistant to various environmental conditions [38, 41]. Silane bonding to inorganic surface is explained in Figure 1.10.

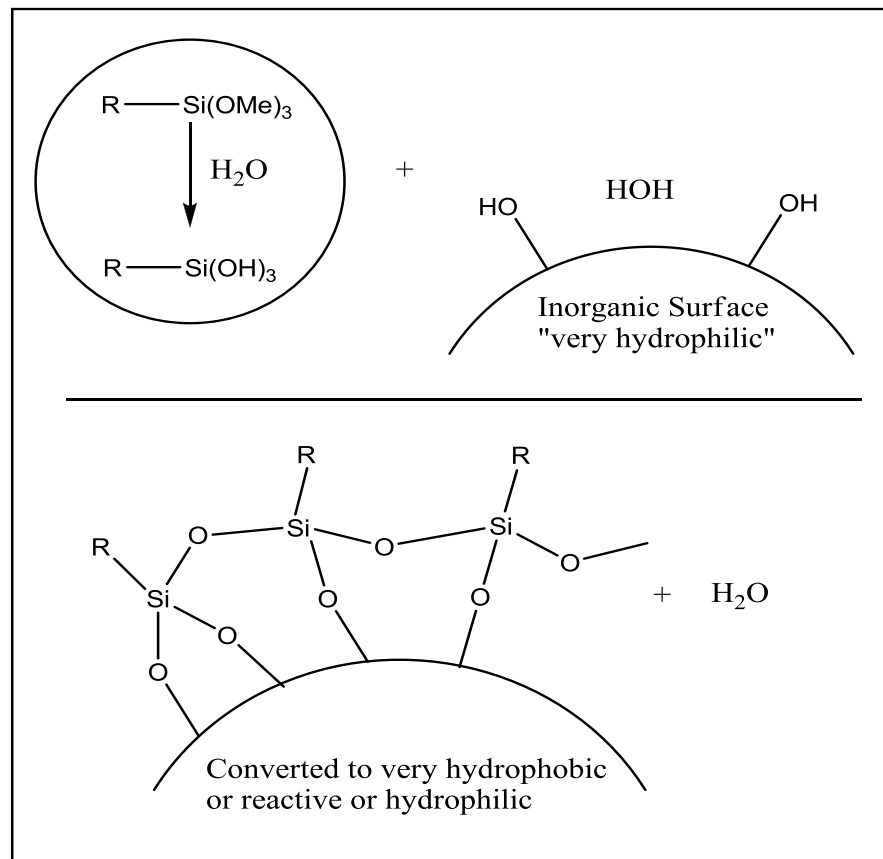


Figure 1.10. Silane bonding to inorganic surface [42].

1.4.1.3. Organofunctional Silanes as Crosslinking Agents Organofunctional end enables the silane to have a chemical or physical interaction with polymer resin. Once silanes are attached to polymer backbone, they are able to form siloxane bonds (Si-O-Si) and link the polymer molecules together. There is need for water or moisture to initiate the hydrolysis of alkoxy group of silane. Water is liberated during condensation of silanols. These hydrolysis/condensation reactions facilitate siloxane bond formation and crosslinking. Silane crosslinking in polymer improves thermal stability, creep resistance, hardness and chemical resistance of coatings, adhesives and sealants. In Figure 1.11 moisture crosslinking of alkoxy silane is given [36, 43].

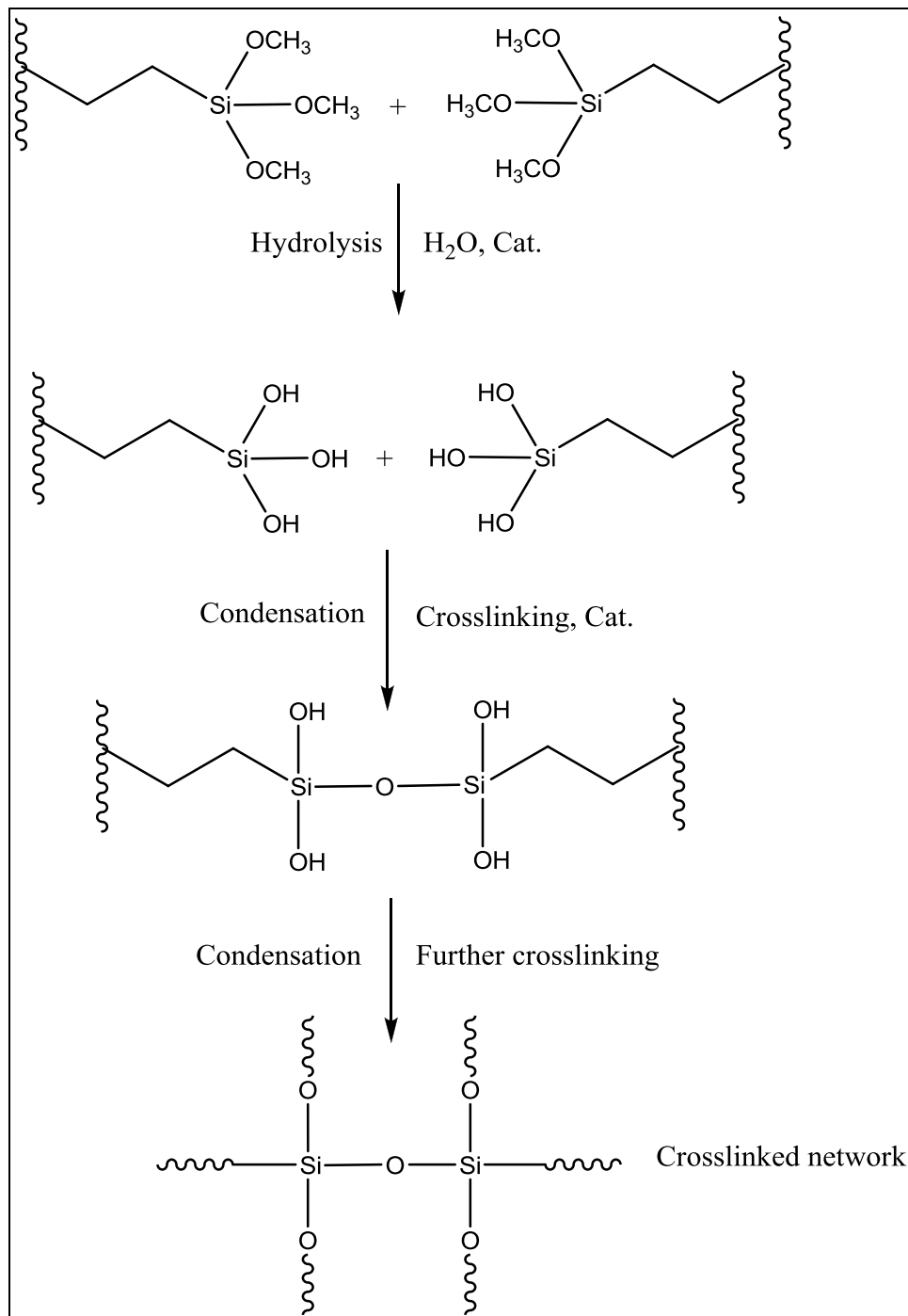
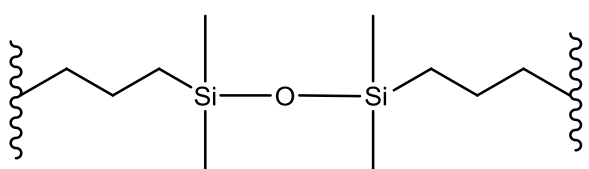


Figure 1.11. Moisture crosslinking of alkoxy silanes [43].

The benefits of moisture curable organofunctional silanes as crosslinkers for use in are explained in Table 1.8.

Table 1.8. The use of silane as crosslinker [41].

 <p>As crosslinker for use in</p>	
Coatings, printing inks	Chemical resistance, corrosion resistance, weatherability, scrub resistance, wet adhesion, release and wetting
Thermoplastics, rubber and elastomers	Elevated temperature application, toughness, abrasion resistance, Rolling resistance, wet electrical properties
Foundry, crude oil, extraction and more...	Core strength

1.4.2. Vinyl Silanes

The organofunctional end of silanes can be used to silylate polymers by either grafting of silane or co-polymerization. The vinyl silanes are the kind of silane that have vinyl group as organofunctional group [36]. In Figure 1.12 the structure of vinyl silane is given.

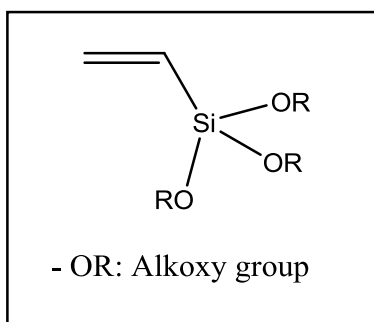


Figure 1.12. The structure of vinyl silane.

One of the several ways to synthesize vinyl silane is zinc-catalyzed nucleophilic substitution reactions of chloro silanes with organomagnesium reagents under mild conditions [44].

As organofunctional group, vinyl functionality allows free radical addition to polymers. Inorganic functional end of vinyl silane bonds to inorganic substrates to provide excellent wet and dry adhesion. These alkoxy groups have fast hydrolysis rate. Vinyl organofunctional silanes can act as crosslinker. The unsaturation can be used to graft silane to various unsaturated polymers via free radical chemistry. The most successful application technique is in polyethylene. The resulting moisture crosslinked material is used as heat shrink tubing in the electrical industry. Polymers such as polyethylene, polyester and styrene-butadiene co-polymers have been grafted with vinyl silane. Silane grafted resin can be crosslinked via an ambient moisture cure mechanism. High temperature resistance, tensile and tear strengths of thermoplastic resin based materials are improved by silane grafting [36].

1.5. Polyethylene Crosslinking and Silane Grafting

The application range of commercial polymers can be increased with a useful way of chemical modification. The modification reactions convert polymers to coupling agents for polymer composites, compatibilizers for polymer blends and precursors for subsequent chemical reactions. For instance, one of the most important chemical modification methods for polyolefin is radical melt grafting of vinyl monomers [45].

Three types of products are manufactured by using polyethylene; pipes, cables and sheets. Polyethylene's service temperature is limited to lower temperature since it is a low melting thermoplastic. This property makes ordinary polyethylene unsuitable for some applications. Thermal stability of polyethylene is increased to resist high service temperature by chemical modifications. This chemical modification is crosslinking [43]. Crosslinking of polyethylene is important in practical applications. It raises the upper

temperature limit of application and improves mechanical properties of polyethylene polymer. Polyethylene has no functional groups that can provide crosslinking ability such as in typical thermosetting resins. The use of silane grafting provides one of several ways of crosslinking. Crosslinking of polyethylene via silane grafting has gained much attention because of its various advantages, such as easy processability, low cost and favorable properties in the processed materials [46-49]. Crosslinked polyethylene gains some improvements in properties such as, increased long term service temperature, increased creep resistance, improved solvent resistance and memory effect. As a result of these improvements, polyethylene is used in a number of applications such as power cable insulation, hot water piping systems and heat shrinkable products [50].

Vinyltrimethoxysilane is the most common silane used in the crosslinkable polyethylene manufacturing. This silane has been introduced into polyethylene by melt grafting in the presence of a peroxide [47]. Polyethylene crosslinking via silane grafting is a thermochemical reaction. Peroxide decomposes and forms oxy radicals at an elevated temperature. These oxy radicals are able to abstract hydrogen atom from polyethylene molecule backbone and attack the vinyl group of silane molecule to convert it into free radicals. The obtained macroradicals either combine with one another or attack another molecule in a similar way to propagate the grafting reaction. This process results in the grafting of vinyl silane onto polyethylene chains. The crosslinking reaction of vinyl silane grafted polyethylene involves hydrolysis of the alkoxy groups with moisture, followed by condensation of the formed hydroxyl groups of silanols to form stable siloxane (Si-O-Si) bonds [43, 45, 49, 51-53].

The degree of crosslinking influences many important properties of crosslinked materials [52]. The extent of vinyl silane grafting to polyethylene increased with increasing amount of silane, reaction time and temperature [48].

In work done by Forsyth, *et al* dodecane was chosen to serve as a model compound for polyethylene in vinyl trimethoxysilane grafting and crosslinking. In Figure 1.13 grafting initiation and propagation of vinyl trimethoxysilane are shown [54]. Parent and colleagues represented studies on the dynamics and yields of peroxide initiated grafting of vinyltriethoxysilane to tetradecane hydrocarbon model compound and polyethylene [55].

In PhD. Thesis by Huttenhower, studied silane grafting to model polyethylene compounds and investigated the fundamental aspects of this reaction; the selectivity, graft distribution, effect of small molecules and mechanism by which this grafting takes place [56].

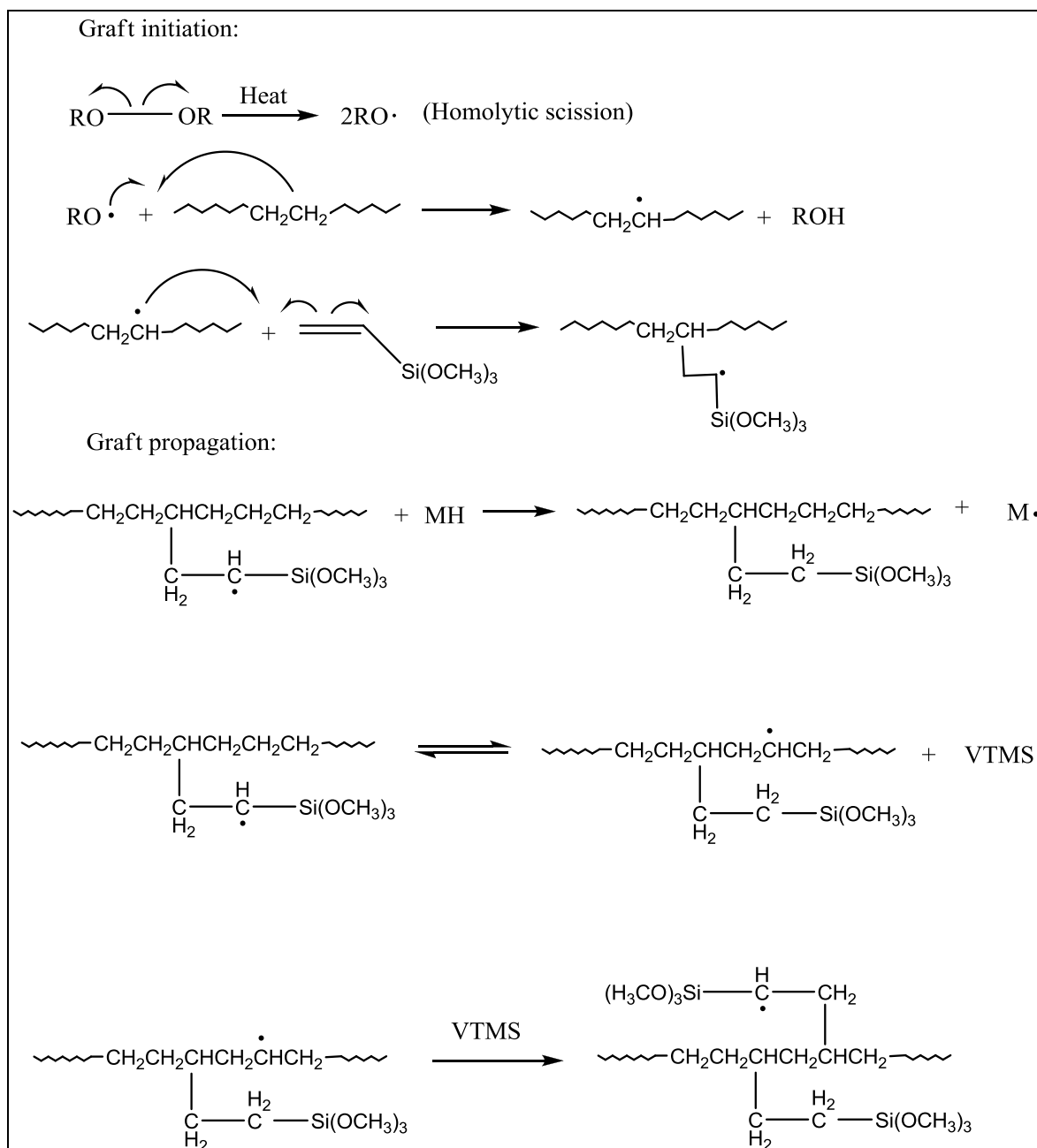


Figure 1.13. Grafting of vinyl trimethoxysilane initiation and propagation steps [54].

2. OBJECTIVES

The aim of the project is to graft vinyl silane to essentially completely saturated triglycerides by using a free radical initiator.

Hydrogenated palm stearin, vinyltrimethoxysilane and dicumyl peroxide are used as reagents.

The chemical structures of the product will be analyzed by ^1H NMR and FTIR spectroscopy, mechanical properties of the homo polymer will be examined and the surface properties of triglyceride coupled glass will be determined.

The product, organosilane derivative of will be hydrolyzed to form silanols. Through condensation of silanol groups, the product react will be homopolymerized or couple with a hydroxyl containing inorganic substrate such as metals or glass surface. The chemical structure of the silanized hydrogenated palm stearin, hydrolysis/condensation and homopolymerization reactions of product are shown in Figure 2.1.

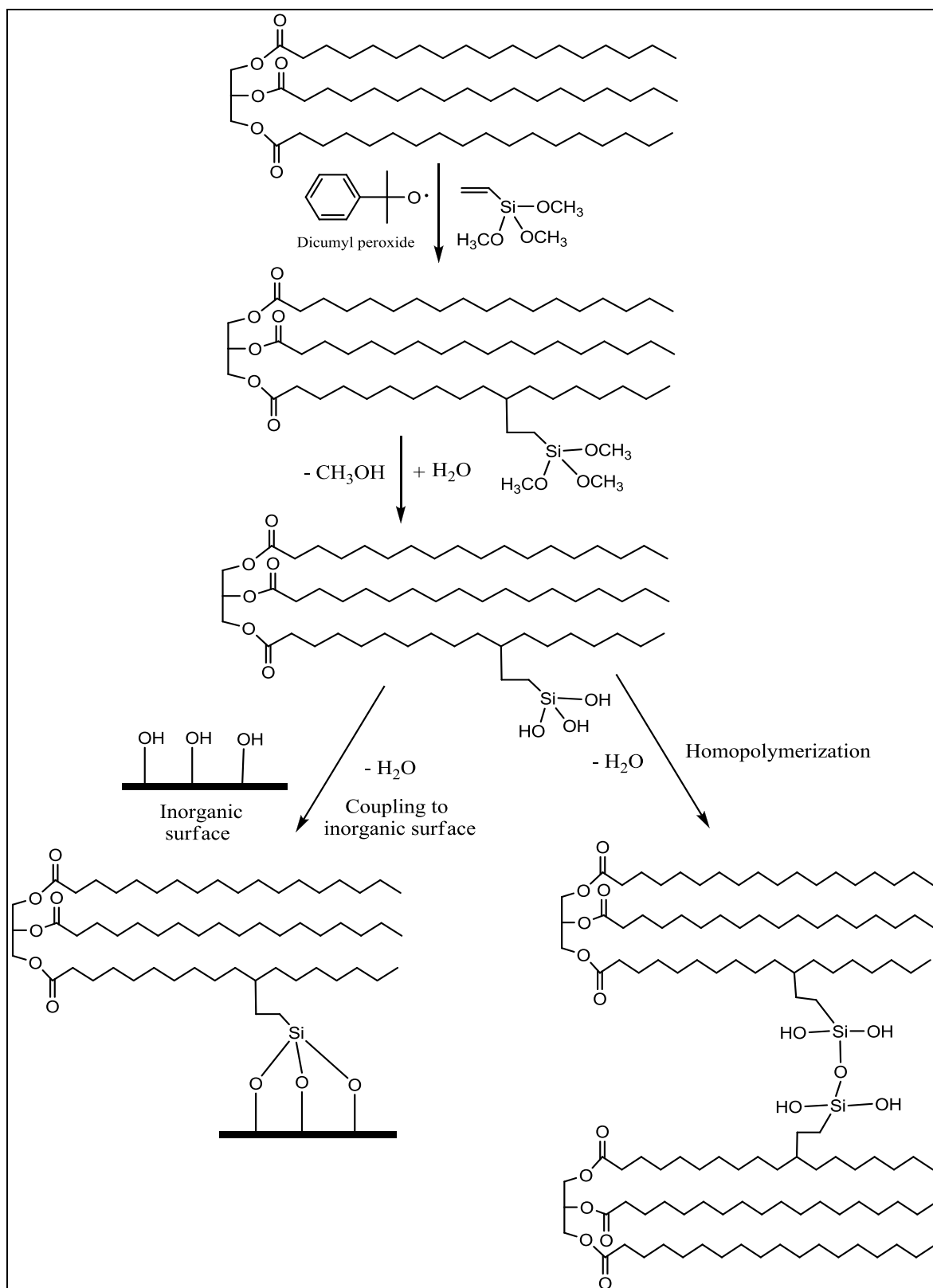


Figure 2.14. Silanized HPS, coupling to inorganic surface and homopolymerization of the product.

3. EXPERIMENTAL

3.1. Materials and Apparatus

3.1.1. Materials

Hydrogenated Palm Stearin (ALEM07RH) (HPS) was obtained from Alemdar Kimya End. A.Ş. (Turkey) and was used without further purification. NMR spectrum shows no vinyl protons. Vinyltrimethoxysilane (Dynasylan Silfin13-VTMS) was obtained from Evonik Industries (Germany) and was used as obtained. The radical initiator Dicumyl peroxide (DCP) was obtained from Pergan the peroxide company (Germany). Deuterated Chloroform (CDCl_3) was obtained from Merck (Germany) and was used for ^1H NMR analysis. Chemical properties of the reagents are given Table 3.1 and Table 3.2.

Table 3.1. Vinyltrimethoxysilane properties.

Dynasylan Silfin 13				
Properties	Test methods	Spec. Limits	Actual values	Units
Dicumylperoxide	SOP 1130	8.0-9.0	8.6	Mass-%
VTMS		> = 88	90	Mass-%

3.1.2. Analytical Instruments

The IR analysis was performed on a Nicolet 380 FT-IR with Smart Diamond ATR.

All the ^1H NMR spectra were recorded on a Varian 400-MHz NMR instrument operating at a frequency of 399.986 MHz for proton. The spectra were reported as a ppm (δ) with TMS as internal standard.

The swelling behavior of the polymers was tested in dichloromethane (CH_2Cl_2) with a Geartner 7109-46 traveling microscope.

The Zwick/Roell Durometer was used to determine the surface hardness of polymer samples, the test was performed according to ASTM D 2240 standart test.

Contact Angle Measurement was performed using KSV CAM 101 contact angle instrument.

The glass transition temperature (T_g) for homopolymer was analyzed by using differential scanning calorimetry (DSC). DSC measurements were carried out with TA Instrument Q 200 at a heating rate of $10\text{ }^\circ\text{C}/\text{min}$ under nitrogen atmosphere.

Table 3.2. Hydrogenated palm stearin properties.

Hydrogenated Palm Stearin	
Name of the analysis	Specidification limts
Appearance	Solid, creamy powder with typical odour
Colour, (Lov. $5^{1/4}$ cell), max	2.0 R/20.0 Y
Moisture, %, max	0.5
FFA, %, (as palmitic), max	1.5
Acid Number, mg KOH/g. max	FFA \times 2.19
Iodine Number, g $\text{I}_2/100$ g, max	1.0
Melting Point, $^\circ\text{C}$	58-60
Chain Distribution, %	
Lauric Acid C 12 max	1.0
Miristic Acid C 14 max	2.0
Palmitic Acid C 16	50-70
Stearic Acid C 18	35-45
Oleic Acid C 18 max	1.0

3.2. Synthesis of Silanized Hydrogenated Palm Stearin

All the glasswares were heated in the oven above 100 °C and they were placed in dessicator during cooling to room temperature to eliminate moisture on glass surface. 3 g of Hydrogenated Palm Stearin (HPS) (0.0034 mol) was placed in a round bottom flask which was equipped with magnetic stirrer and heated to 112 °C. Flask was sealed with rubber septum. Dry nitrogen gas (N₂) was led into the flask to remove any residual moisture. 2.5 g of Vinyltrimethoxysilane (VTMS) (0.0168 mol) and 0.15 g of Dicumylperoxide (DCP) (5% by weight based on hydrogenated palm stearin) were added to flask dropwise as a solution in 30 min. HPS, VTMS and DCP were stirred at 112 °C for 40 hours under nitrogen gas to achieve at least 4 half lives of the peroxide (Half life of DCP at this temperature is 10 hours)[57]. After 40 hours, in order to remove unreacted VTMS, N₂ gas was led into the flask. Final product was white, moisture sensitive solid at room temperature. The characterization of the final product was done with ATR-IR and ¹H NMR spectroscopy.

ATR-IR (cm⁻¹): 2955, 2916, 2849 (s, C-H, stretching), 1740 (s, C=O, ester carbonyl stretch), 1728 (m, C=O, stretch), 1464 (m, CH₂, Def.), 1173 (m, C-O-C, Def.), 1195 (m, C-O-C, Def.), 1085 (s, Si-O-C, asymmetric stretching), 969 (w, Si-O-C, symmetric stretching), 812, 767 (w, =C-H and =CH₂ out of plane bending), 719 (w, CH₂ rocking).

¹H NMR (CDCl₃, 400 MHz) ppm: 0.58 (-CH₂-Si-), 0.88 (-CH₃), 1.24 (-CH₂-), 1.3 (-CH₂-CH₂-Si-), 1.32 (-CH₂-CH₃), 1.47 (-CH-CH₂-CH₂-Si-), 2.30 (-O(C=O)CH₂-), 3.55 (-Si-OCH₃), 4.26 (-O-CH₂-CH(O-)-CH₂-O-), 5.24 (-O-CH₂-CH(O-)-CH₂-O-)

3.3. Homopolymerization of Silanized Saturated Fat via Moisture Curing

Silanized product was kept in a moisture chamber to allow hydrolysis of methoxysilane groups for 24 hours. The curing process was done at 125 °C for 12 hours. The polymeric product of silanized hydrogenated palm stearin was light yellow in colour and brittle, rubbery material at room temperature. Since the polymer is not soluble in any

solvent, it is not possible to perform NMR analysis. The characterization is done with IR spectroscopy.

ATR-IR (cm^{-1}): 2956, 2916, 2849 (s, C-H, stretching), 1739 (s, C=O, stretch), 1466 (m, CH_2 , Def.), 1195 (m, C-O-C, Def.), 1170 (m, C-O-C, Def.), 1092 (m, Si-O-C, asymmetric stretching), 1049, 1026 (m, Si-O-Si, stretching), 720 (m, CH_2 , rocking).

3.4. Surface Characterization of Silanized Saturated Fat Grafted Glass

3.4.1. Contact Angle Measurement

Solution casting was done on glass surface with VTMS grafted HPS dissolved in tetrahydrofuran (THF). Contact angles of water droplets were measured on the both side of the drop by the sessile drop method at room temperature. Ten measurements were taken at the different positions on the glass surface and the average values were reported as contact angle.

3.5. Swelling Test

Rectangular shaped pieces of polymer samples of dimensions approximately $1 \times 5 \times 10$ mm were used for the swelling test. The samples were put in a closed container filled with CH_2Cl_2 as solvent. The increase in the lengths was measured with one hour time interval until solvent uptake ceased. For each sample tests were repeated and average values were recorded as result.

4. RESULTS AND DISCUSSION

4.1. Characterization and Qualitative Analysis of Hydrogenated Palm Stearin

Saturated fats that are obtained from animals and plants contain some unsaturation and have iodine values around 30. Grafting of vinyl silane to unsaturated triglyceride has been reported [4, 58]. In order to prevent grafting of vinylsilane on these double bonds, fully hydrogenated palm stearin was used in this work. Hydrogenated Palm Stearin (HPS) (ALEM07RH) was obtained from Alemdar Kimya End. A.Ş. Characterization and qualitative analysis of the HPS was done by using ^1H NMR and FT-IR analysis.

In Figure 4.1, the chemical structure and ^1H NMR spectrum of HPS are given. The characteristic peaks of HPS are explained. The peak (a) appearing at 0.8 ppm corresponds to methyl ($-\text{CH}_3$) protons of the end groups of fatty acid chains. The peak (b) at 1.2 ppm corresponds to $-\text{CH}_2-$ protons of fatty acids, peak (c) at 1.6 ppm belongs to β protons ($-\text{CH}_2-$) of the ester, peak (d) appearing at 2.2 ppm corresponds to protons α to the carbonyl, peak (e) appearing in the 4.0-4.4 range corresponds to $-\text{CH}_2$ protons of the glycerol unit. Peak (f) appearing at 5.3 ppm corresponds to $-\text{CH}-$ proton of the glycerol unit. There are no peaks appearing at 6.0 ppm which belong to vinyl protons of the unsaturation. This proves there are no unsaturations present in HPS.

FT-IR spectrum of hydrogenated palm stearin is shown in Figure 4.2. There are no peaks appearing at 1655 cm^{-1} corresponding to carbon carbon double bond absorptions. A very small peak that may be due to vinyl hydrogens appears at 2956 cm^{-1} . FT-IR results coincide with NMR results that there is no unsaturation present on the back bone of the HPS.

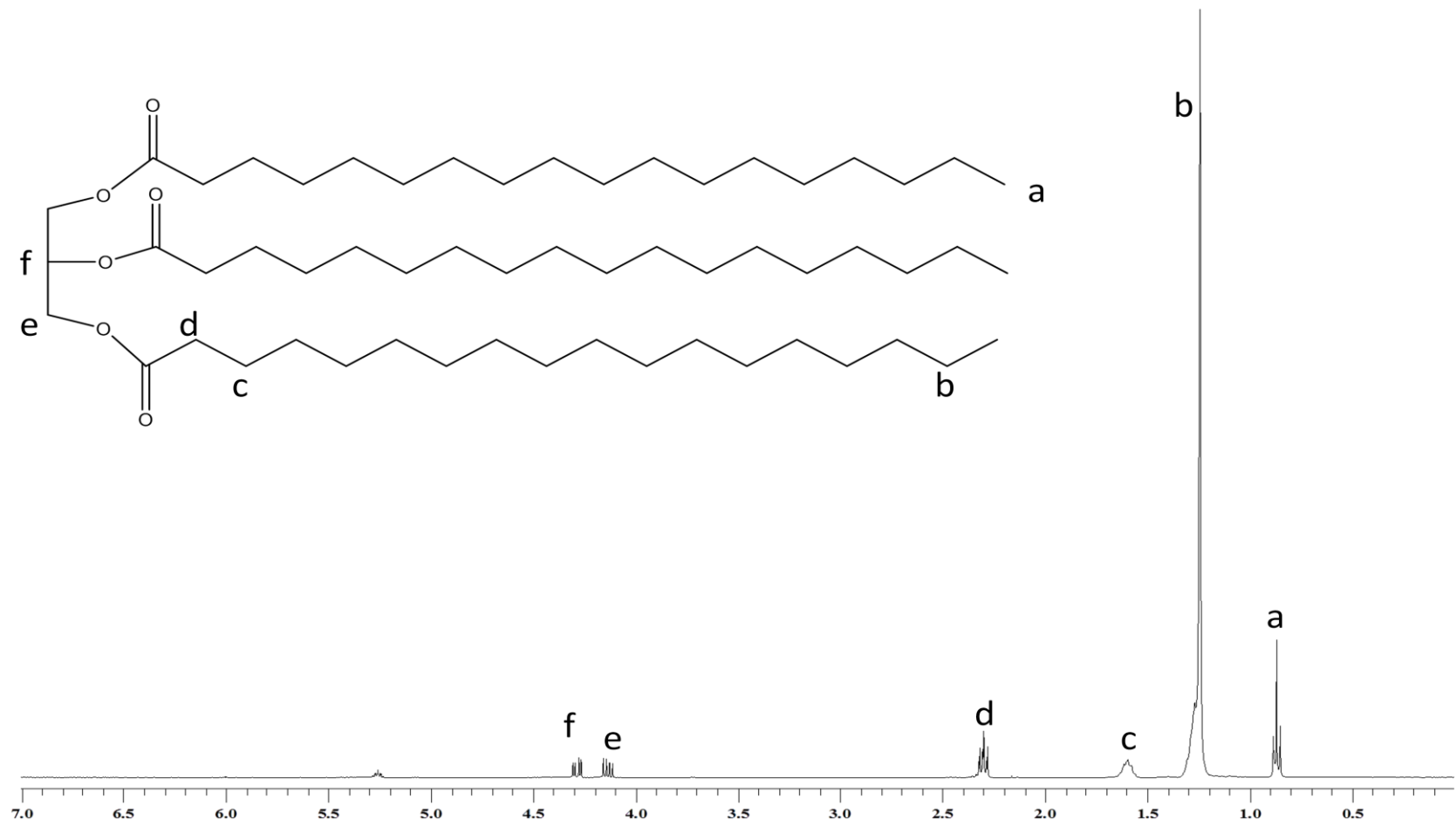


Figure 4.1. ¹H NMR spectrum of hydrogenated palm stearin.

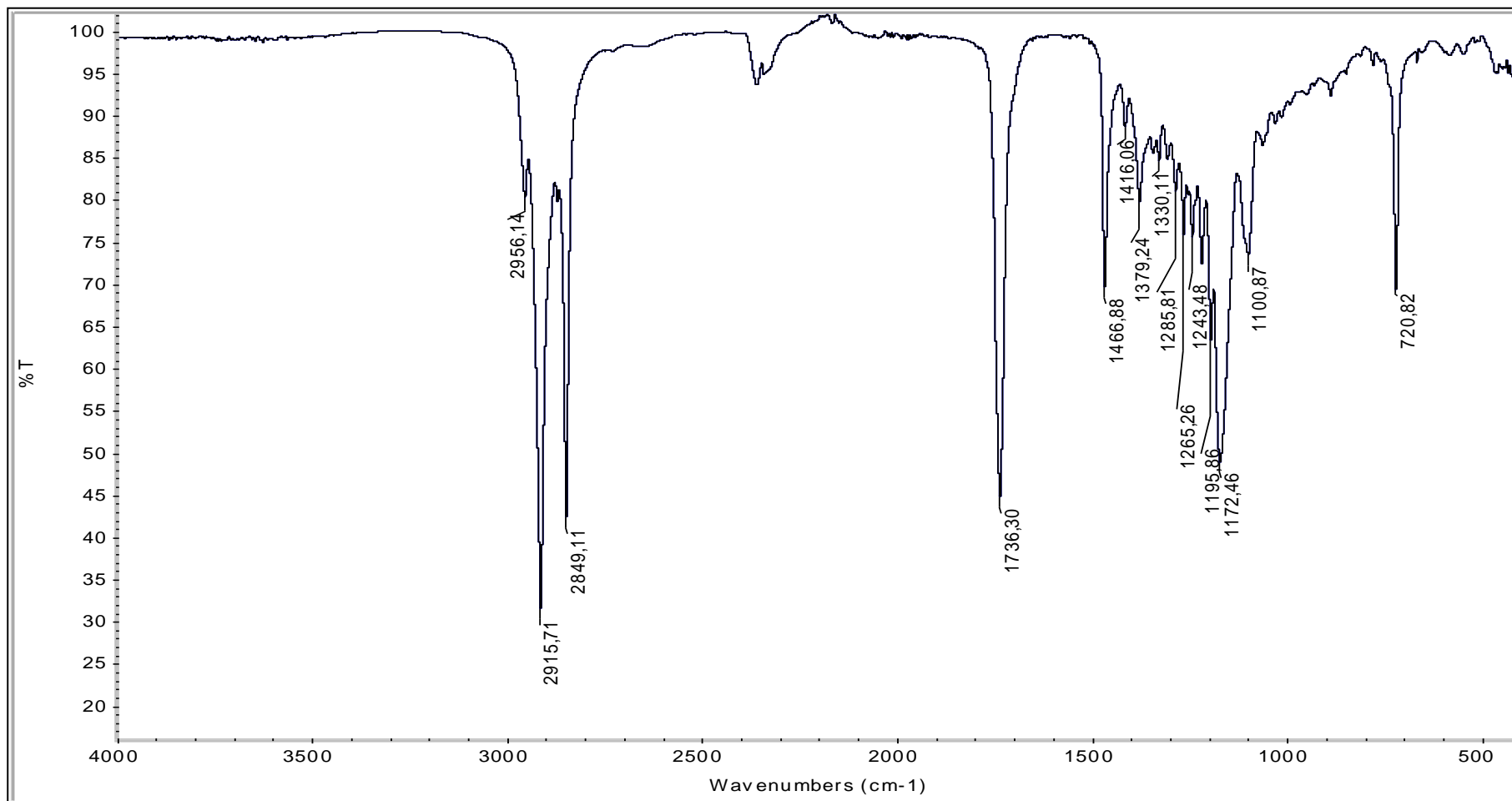


Figure 4.2. FTIR spectrum of hydrogenated palm stearin.

4.2. Synthesis and Characterization of Silanized-HPS

As stated in work done by Forsyth et al. [54], the peroxide initiated grafting of vinyltrimethoxysilane (VTMS) onto dodecane has been successful. This reaction was chosen as a model for grafting VTMS onto HPS. Dodecane is an alkane which has no functional groups. These chemical properties of dodecane resemble the fatty acid chains of saturated triglyceride. Peroxide used in the experiment decomposes and forms alkoxy radicals. In the case of dicumyl peroxide (DCP), these radicals have bulky benzene ring. These bulky groups cause steric hindrance and such radicals undergo addition to vinyl groups very slowly. However their hydrogen abstraction is quite fast. Decomposition of dicumyl peroxide is shown in Figure 4.3.

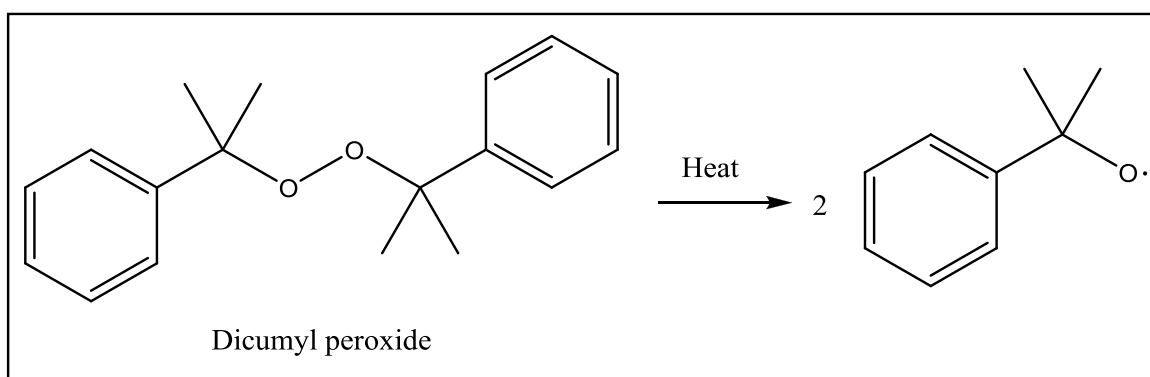


Figure 4.3. Dicumyl peroxide decomposition.

The reaction initiation step occurs when an alkoxy radical formed from decomposition of dicumyl peroxide initiator as shown in Figure 4.3 and abstracts a hydrogen from the hydrocarbon chain. This hydrocarbon radical then reacts with VTMS to form a single grafted radical intermediate. After this, propagation step can then continue by one of the three methods as shown in Figure 4.4. (i) intermolecular abstraction, hydrocarbon radical abstracts a hydrogen atom from another hydrocarbon chain, (ii) intramolecular abstraction, back biting or 1,5 hydrogen shift a hydrogen atom is abstracted from another carbon atom on the same hydrocarbon chain. 1,5 hydrogen-shift mechanism in VTMS graft propagation is shown in Figure 4.5. (iii) homopolymer grafting (oligomeric grafting) hydrocarbon radical grows by adding to another VTMS [56].

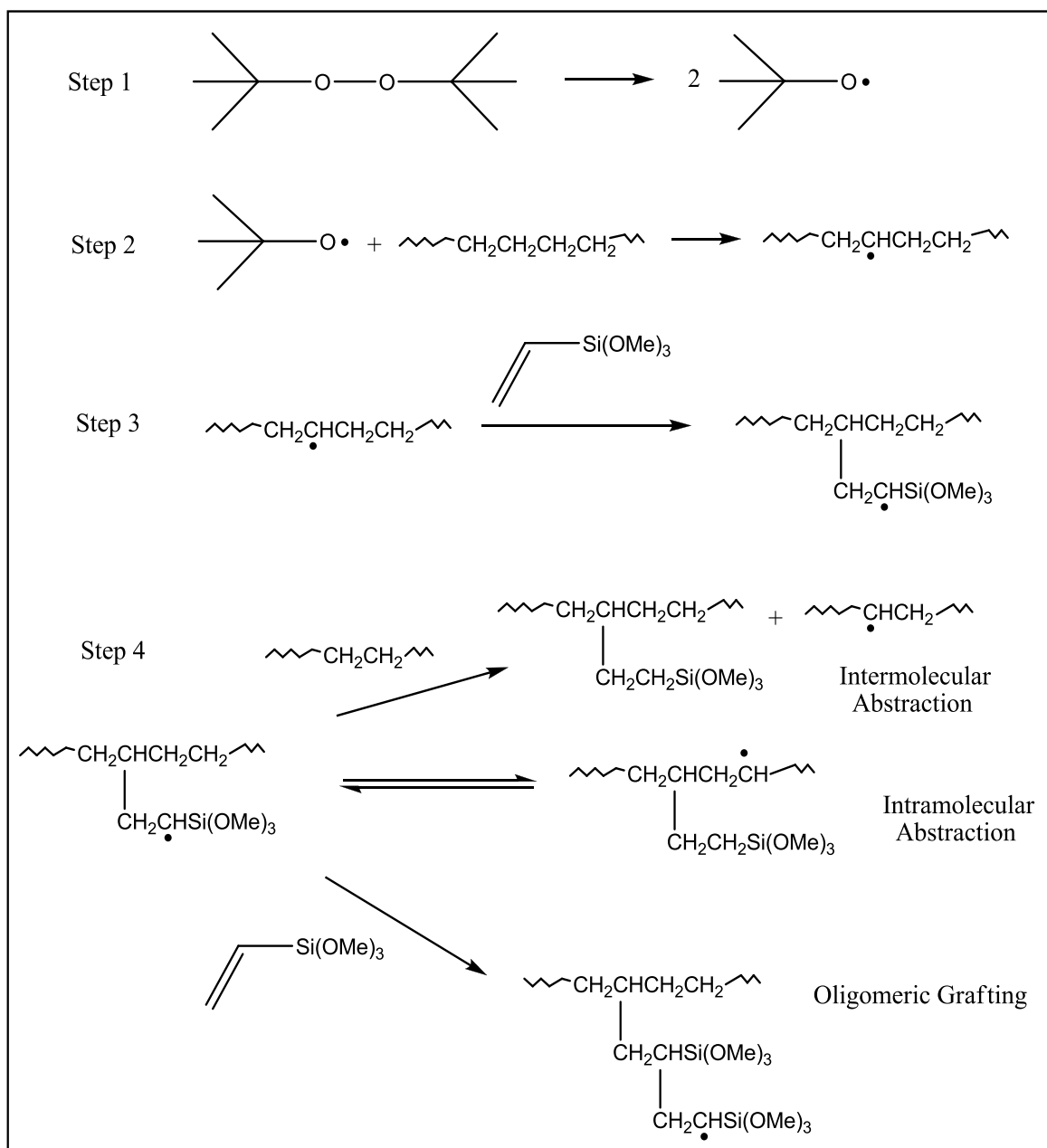


Figure 4.4. Vinyltrimethoxysilane grafting onto a hydrocarbon chain by the peroxide initiated radical method [59].

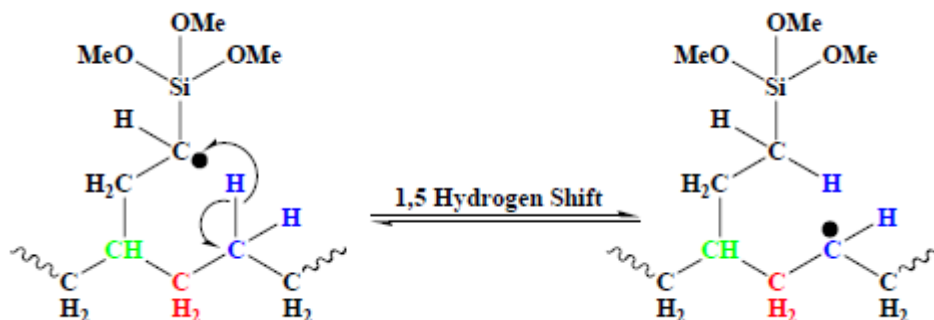


Figure 4.5. 1,5 Hydrogen-shift mechanism [56].

In Figure 4.6, the chemical structure and ^1H NMR spectrum of VTMS are given. Dynasylan Silfin-13 a commercial product is used as vinylsilane in this work. It contains Dicumylperoxide (DCP) in its formulation at a certain ratio. Corresponding peaks of DCP are shown in ^1H NMR. The peak (a) appearing at 1.36 ppm and the peak (b) at 1.49 ppm correspond to methyl ($-\text{CH}_3$) protons of DCP. The peak (h) appearing at 7.16 ppm and the peak (g) at 7.36 ppm belong to ($=\text{CH}$) protons of benzene ring DCP. The peak (c) appearing at 3.53 ppm corresponds to methyl ($-\text{CH}_3$) protons of the silane. Vinylic hydrogen atoms ($=\text{CH}$) give characteristic peaks as peak (d) at 5.80 ppm, peak (e) 5.94 ppm and peak (f) 6.09 ppm.

In Figure 4.7, IR spectrum of VTMS is shown. The peak appearing at 3062 cm^{-1} and 1599 cm^{-1} correspond to carbon carbon double bond absorption peaks. Strong absorption bands are observed at 1075 cm^{-1} and 1190 cm^{-1} corresponding to the asymmetric stretching of the Si-O-C group. Symmetric stretching of the same group appearing at 967 cm^{-1} . The peak appearing at 808 cm^{-1} and 765 cm^{-1} correspond to $=\text{CH}_2$ and $=\text{CH}$ out of plane bending.

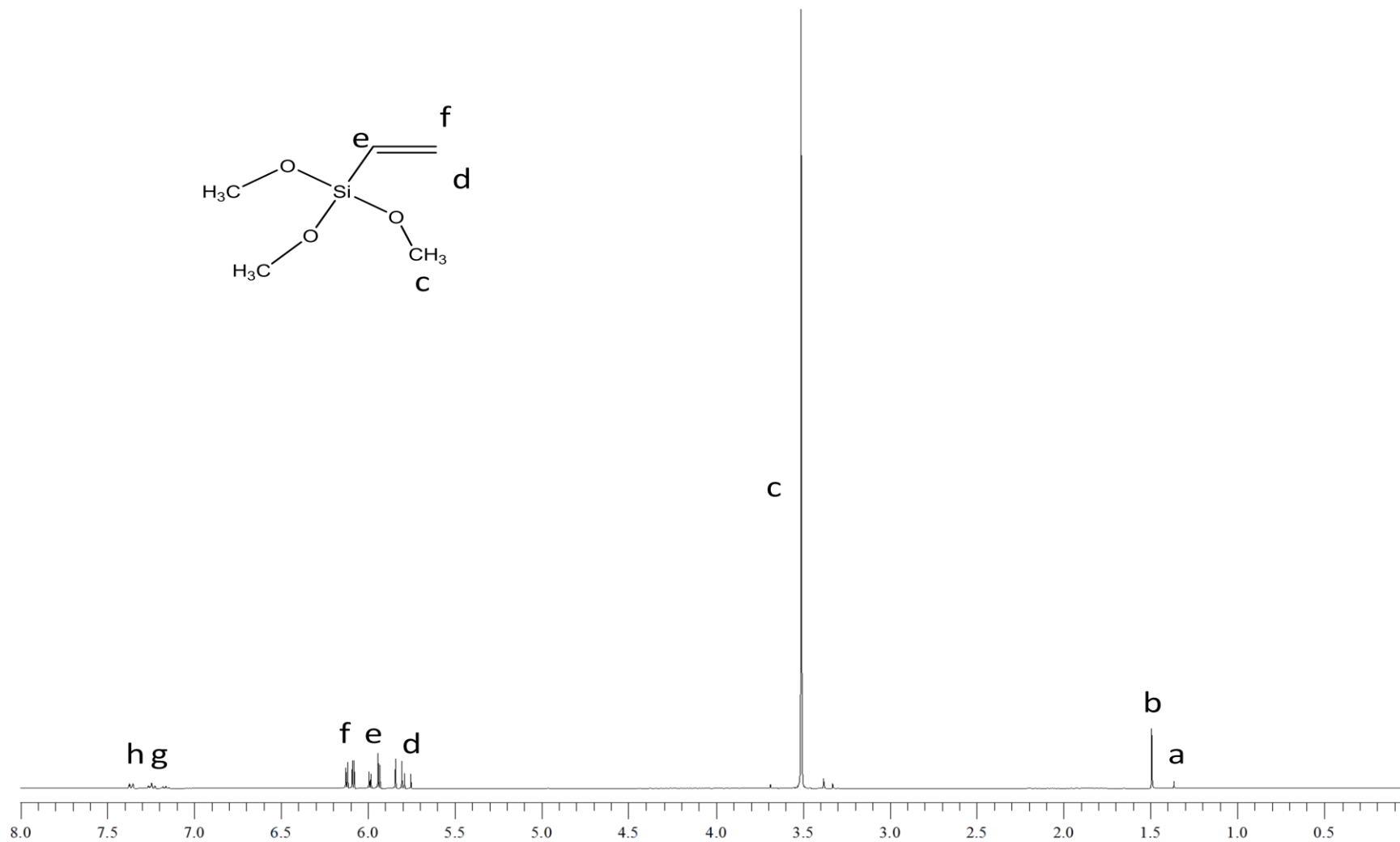


Figure 4.6. ^1H NMR spectrum of vinyltrimethoxysilane.

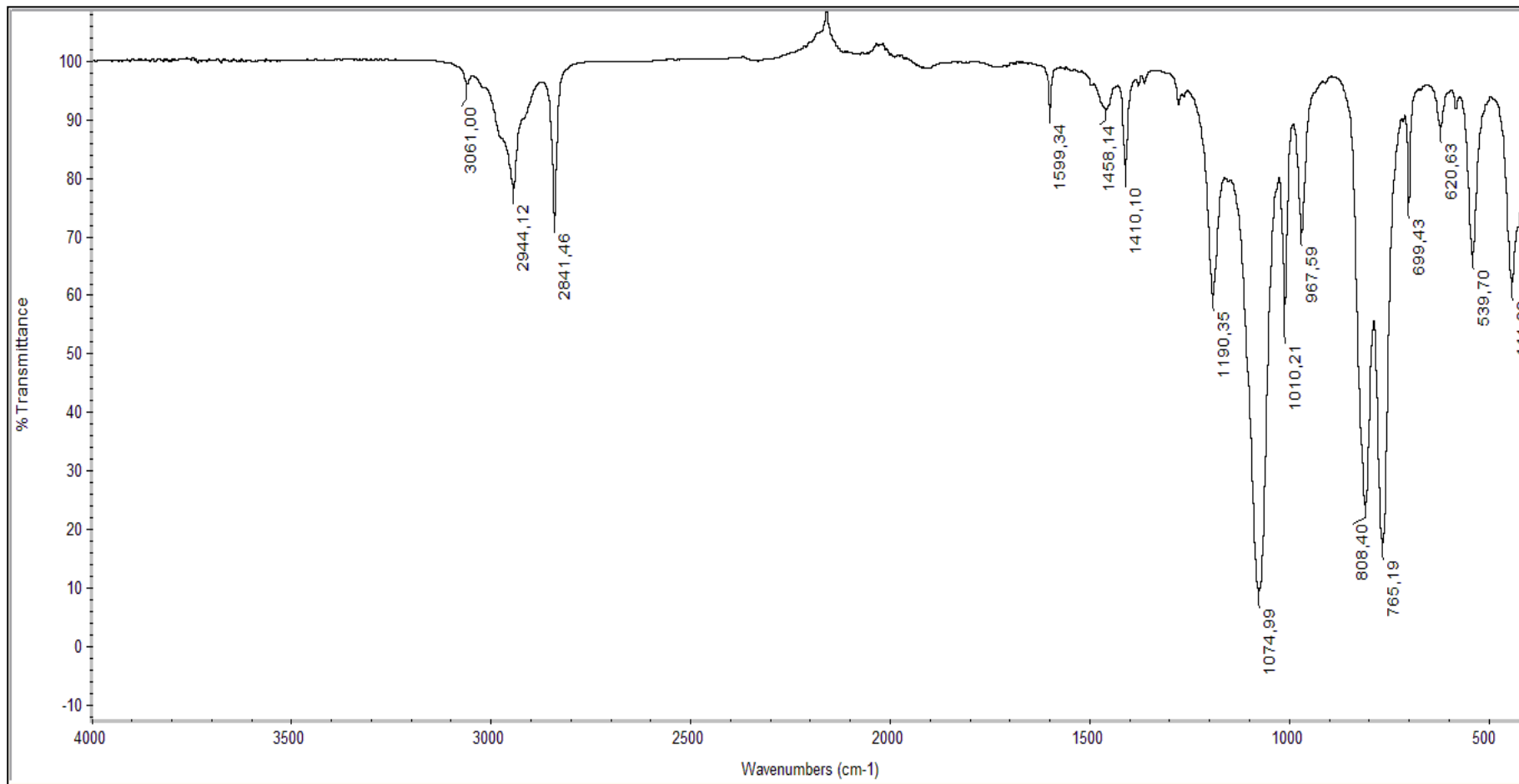


Figure 4.7. FTIR spectrum of vinyltrimethoxysilane.

Vinylsilane acts as a coupling agent between an unsaturated organic polymer and an inorganic surface or a filler as explained in Section 1.4.2. Vinylsilane is an organofunctional silane having both organic reactive (vinyl) and inorganic reactive (silanol) end. In the presence of sufficient amount of water, methoxy end of the molecule can be hydrolyzed to silanols that can either react with hydroxyl bearing inorganic surfaces such as glass or metals or homopolymerize itself with other silanols. Figure 4.8 shows the chemical structure of the silanized-HPS. Although only one VTMS graft is shown in the figure, it is understood that more than one VTMS can be grafted to the same or different fatty acids in the triglyceride.

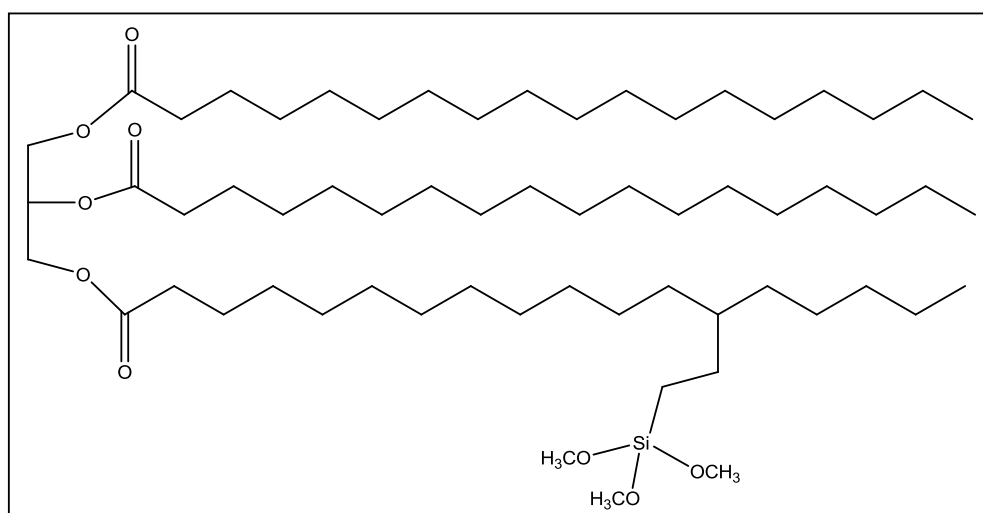


Figure 4.8. Structure of silanized-HPS.

The important point of the grafting reaction is that all the precautions must be taken to prevent presence of water. Because methoxy groups of silane molecule are known to be very sensitive to moisture. Moisture on the surface of the glassware and moisture present in air can be enough to hydrolyze these alkoxy groups [39] and cause premature condensation reactions.

The boiling point of vinyltrimethoxysilane is 123 °C and the melting point of HPS is 58 °C. The reaction temperature is chosen 112 °C which is above the melting of HPS but very close to boiling point of VTMS. The higher temperature was chosen so that DCP could decompose and three half lives of the peroxide could be achieved in a reasonable

time. Half live of DCP at 112 °C is 10 hours [60]. Extreme care was taken for keeping the reaction media dry. Before the addition of the reagents, nitrogen gas was purged to flask. The reaction was done by mixing 5:1 mole ratio of VTMS and HPS. VTMS was in excess because triglyceride of saturated fat has 3 fatty acid chains and the reaction temperature was close to boiling point of VTMS, some of the vinylsilane could evaporate, some was condensed on the glass surface of flask and did not take place in the reaction. After the reaction, nitrogen gas was led to the flask to evaporate the unreacted VTMS from the reaction media.

NMR and IR spectroscopy techniques were used in the characterization of the silanized-HPS. FTIR spectra of the silanized-HPS is given in Figure 4.9. Figure 4.10 shows the ^1H NMR of the product. The trimethoxysilyl group gives characteristic absorptions at 793 and 1089 cm^{-1} . These absorptions were present in the IR spectrum of the silanized-HPS and correspond to $-\text{Si-O-C}-$ stretching. ^1H NMR spectrum in Figure 4.10 shows, complete disappearance of the peaks corresponding to $-\text{CH}_2=\text{CH}$ protons of the vinyltrimethoxysilane indicated that there is no unreacted vinylsilane left in the reaction media. The appearance of the peak at 1.47 ppm corresponds to $-\text{CH}$ protons where the grafting of vinylsilane to HPS occurred. The peak appearing at 3.55 ppm corresponds to $(-\text{Si-O-CH}_3)$ and this proved that vinylsilanes were not hydrolyzed.

In order to calculate the number of functional methoxysilane groups present in one molecule of HPS, the ratio of integral value of the peak corresponding to methyl protons of at the end of the fatty acid chains (a) to the integral value of the peaks corresponding to $(-\text{O-CH}_3)$ methoxy protons (f) was calculated. From that ratio it was concluded that there are on the average of 0.82 methylsilane functional groups per triglyceride. This clearly means there is considerable unreacted HPS in the mixture. In the light of moisture sensitivity of the product, the unreacted HPS could not be extracted without causing considerable hydrolysis of the methoxy group of silane. The problem was solved by first polymerizing the VTMS adduct and then removing the unreacted triglyceride from the polymeric product.

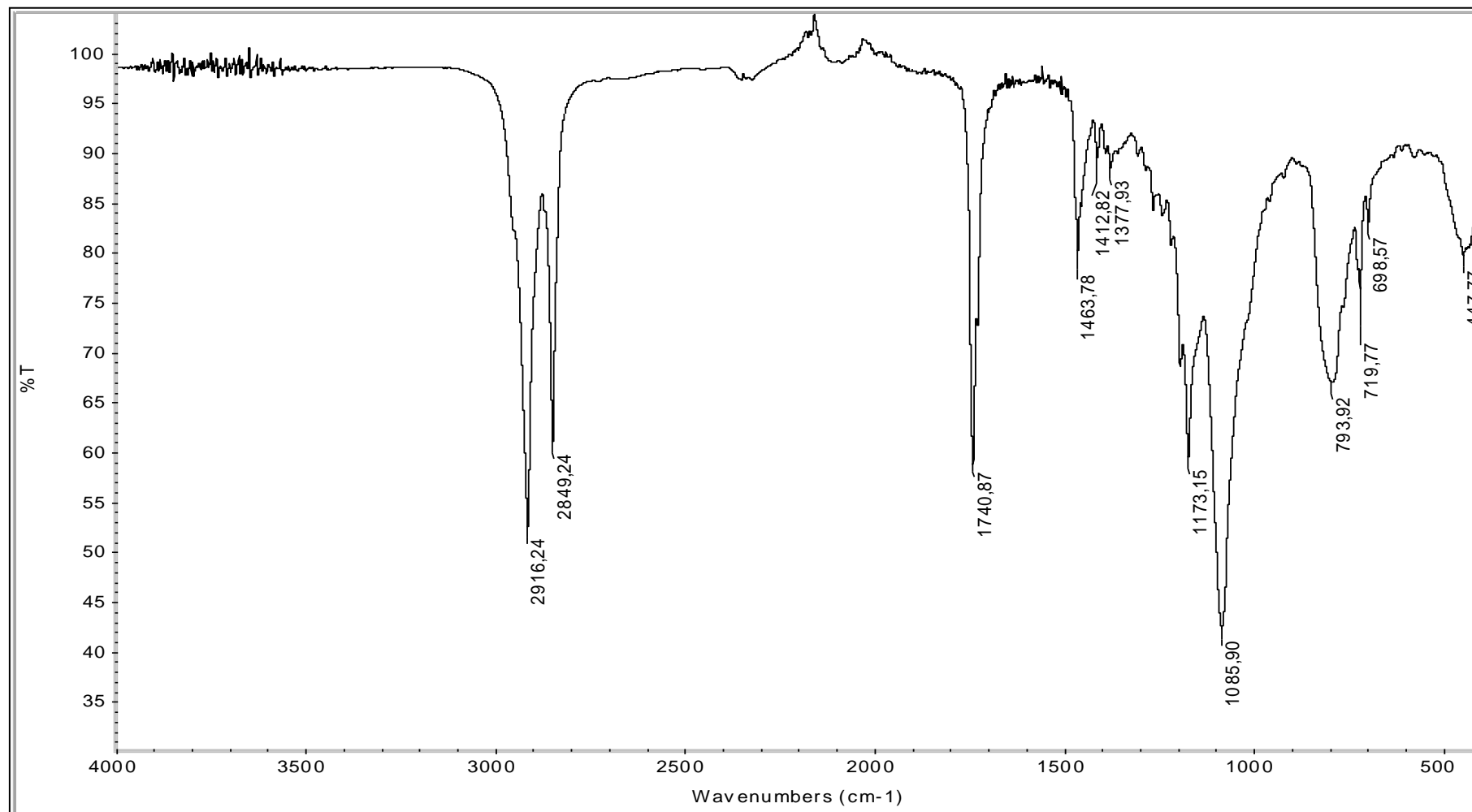


Figure 4.9. FTIR spectrum of vinyltrimethoxysilane grafted HPS.

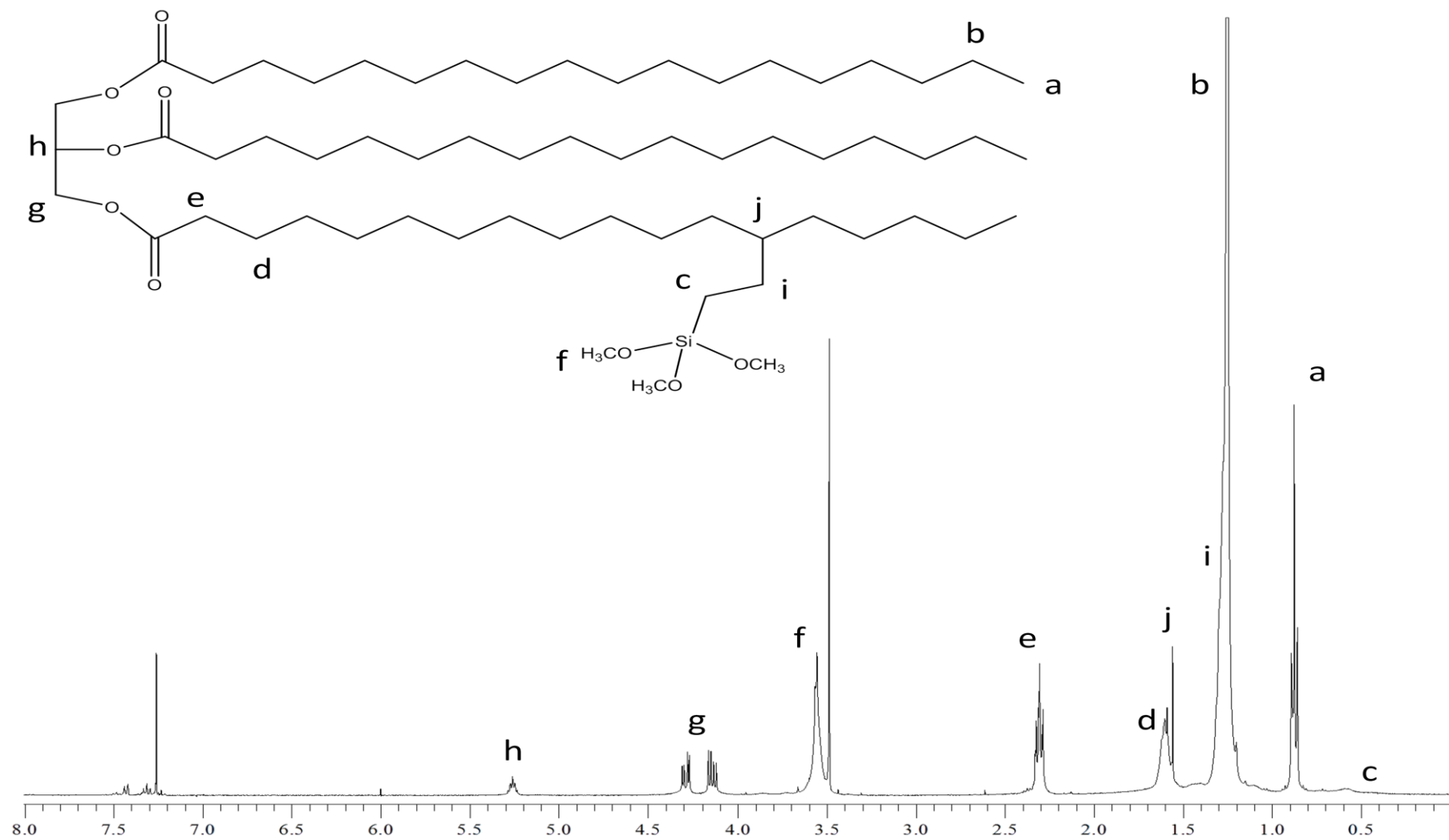


Figure 4.10. ^1H NMR spectrum of vinyltrimethoxysilane grafted HPS.

4.3. Homopolymerization of Silanized-HPS

The uses of organofunctional silanes are explained in Section 1.4.1. Homopolymerization of vinyltrimethoxysilane grafted hydrogenated palm stearin was done by moisture curing. In the presence of adequate moisture, the polymer sample was kept for 24 hours to allow methoxysilane groups to hydrolyze. After hydrolysis, the sample was heated further for condensation. Water was consumed during hydrolysis and given out during condensation. The hydrolysis/condensation of the polymer is an equilibrium. Adequate temperature and water will promote silanol formation and for condensation polymer must be heated to a temperature around 100 °C to push the silanol-silyl ether equilibrium to the right by methanol and water evaporation. In work done by Shah and colleagues [43], the catalyst (dibutyl tin dilaurate) was used to reduce the activation energy for the hydrolysis of the alkoxy groups of the silane molecules and after hydrolysis condensation of silanols (OH groups) was favored by catalyst. Hydrolysis of the trimethoxysilane liberates three silanol groups therefore even a molecule of triglyceride with a single VTMS graft is trifunctional. Such trifunctional molecules are capable of polymerizing and crosslinking. The IR spectrum of the polymerized product shows no -OH absorptions after post curing. Therefore it can be assumed that all silanols have been used in the polymerization/crosslinking reaction. This crosslinking reaction is shown in Figure 4.11.

Moisture curing of polymer resulted with covalent (Si-O-Si) bond formation from hydroxysilane groups. These covalent bonds have 598kJ/mol bond strength. Characterization of the silanized-HPS homopolymer was done by IR spectroscopy. Figure 4.12 shows the IR spectra of moisture cured silanized - HPS. Si-O-Si bond appears as a shoulder in 1030 cm^{-1} . The peaks corresponding to Si-O-C and Si-O-Si stretching are both appear in the same region.

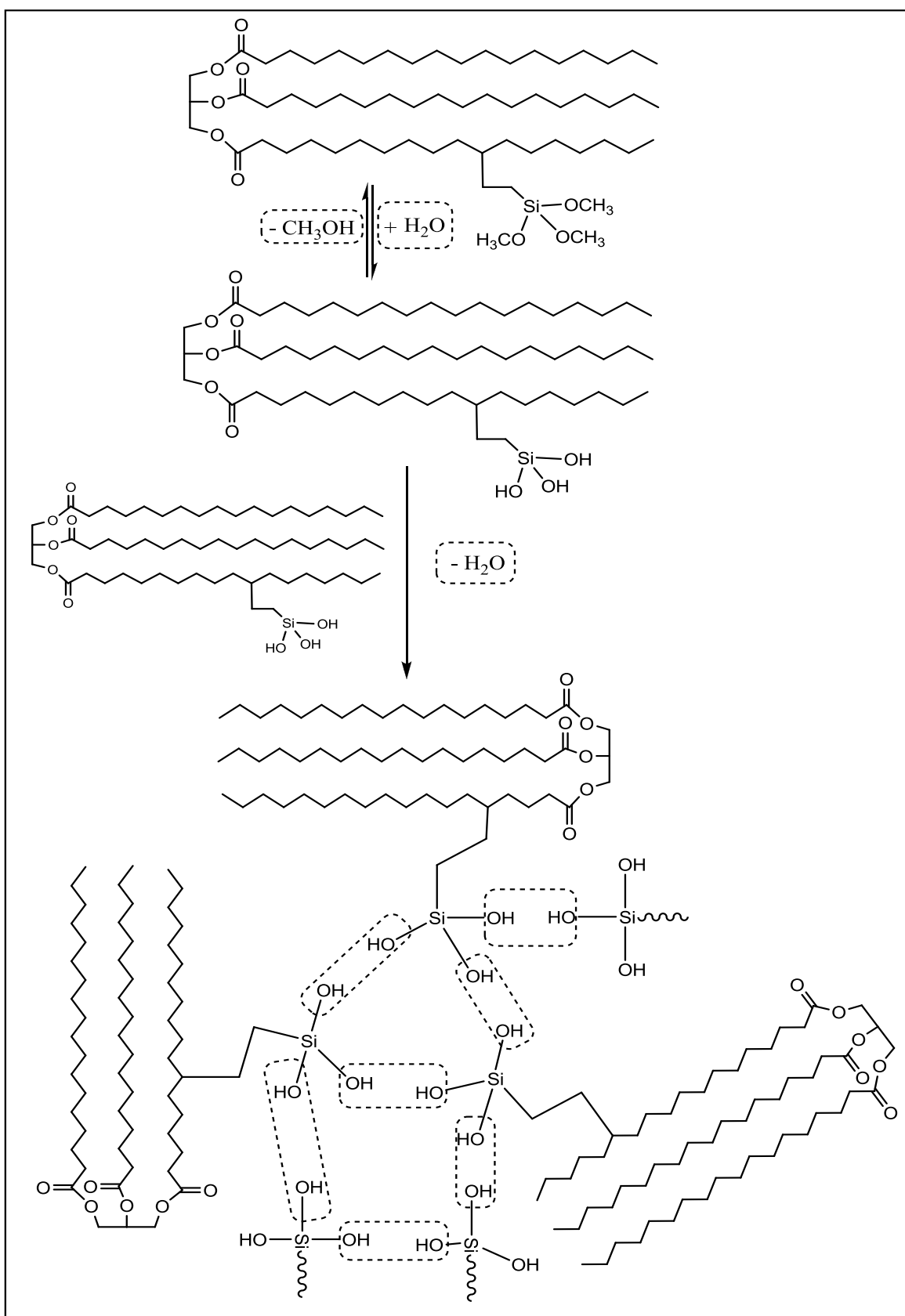


Figure 4.11. Crosslinking reaction of VTMS γ HPS.

The homopolymer of VTMS γ HPS has very poor mechanical properties. Especially the fracture toughness of the samples are so low that they cannot be removed from the mold without fracturing. Therefore no mechanical property test could be performed on these samples by using Dynamic Mechanical Analysis technique. Only thermal analysis, surface hardness and swelling tests could be performed. Homopolymerized VTMS γ HPS contains considerable amount of unreacted HPS. This probably contributes to the poor mechanical properties of the sample. After polymerization samples were extracted with dichloromethane and the IR spectra of the extracted sample and the extract are shown in Figure 4.13 and Figure 4.14. The extracted sample shows essentially the same IR spectrum as VTMS γ HPS as the material removed is unreacted HPS having the same functional groups as VTMS γ HPS. The extract shows only HPS.

Numerous attempts were made to increase the grafting efficiency. There are listed below:

- (i) The mole ratio of VTMS:HPS is set to 5:1. VTMS was used in excess amount.
- (ii) The reaction temperature is set to 112 °C below the boiling point of VTMS.
- (iii) The reaction was continued for 40 hours in order to achieve 4 half lives of peroxide.
- (iv) Reaction was carried out in a sealed round bottom flask under nitrogen atmosphere to prevent any moisture presence.
- (v) VTMS and DCP were added to HPS drop wise at reaction temperature.
- (vi) DCP was added to a mixture of VTMS and HPS drop wise.
- (vii) VTMS, HPS and DCP were mixed in a sealed tube before heating to prevent any moisture.

None of these methods gave a measurable increase in grafting efficiency.

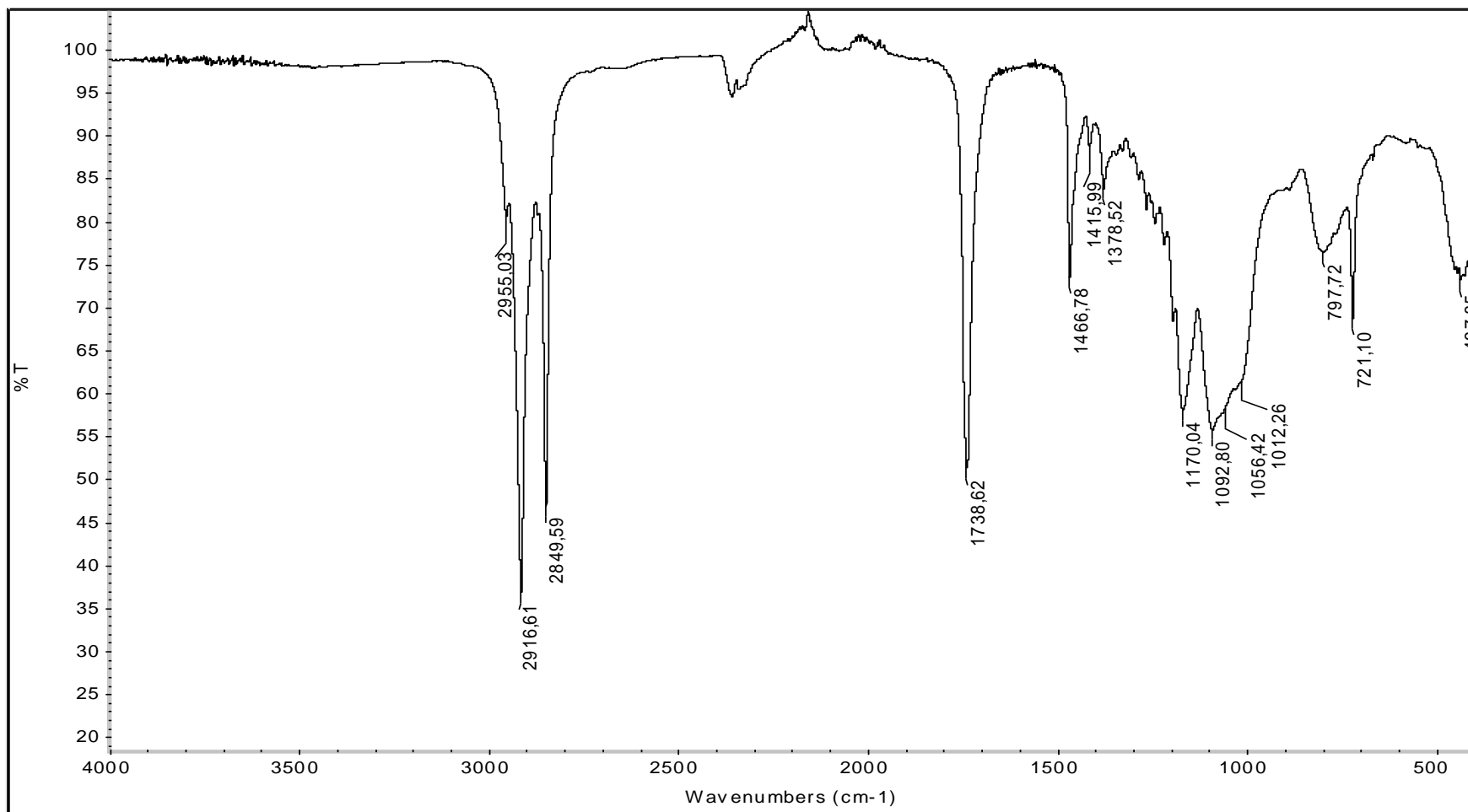


Figure 4.12. FTIR spectrum of homopolymer VTMS grafted HPS.

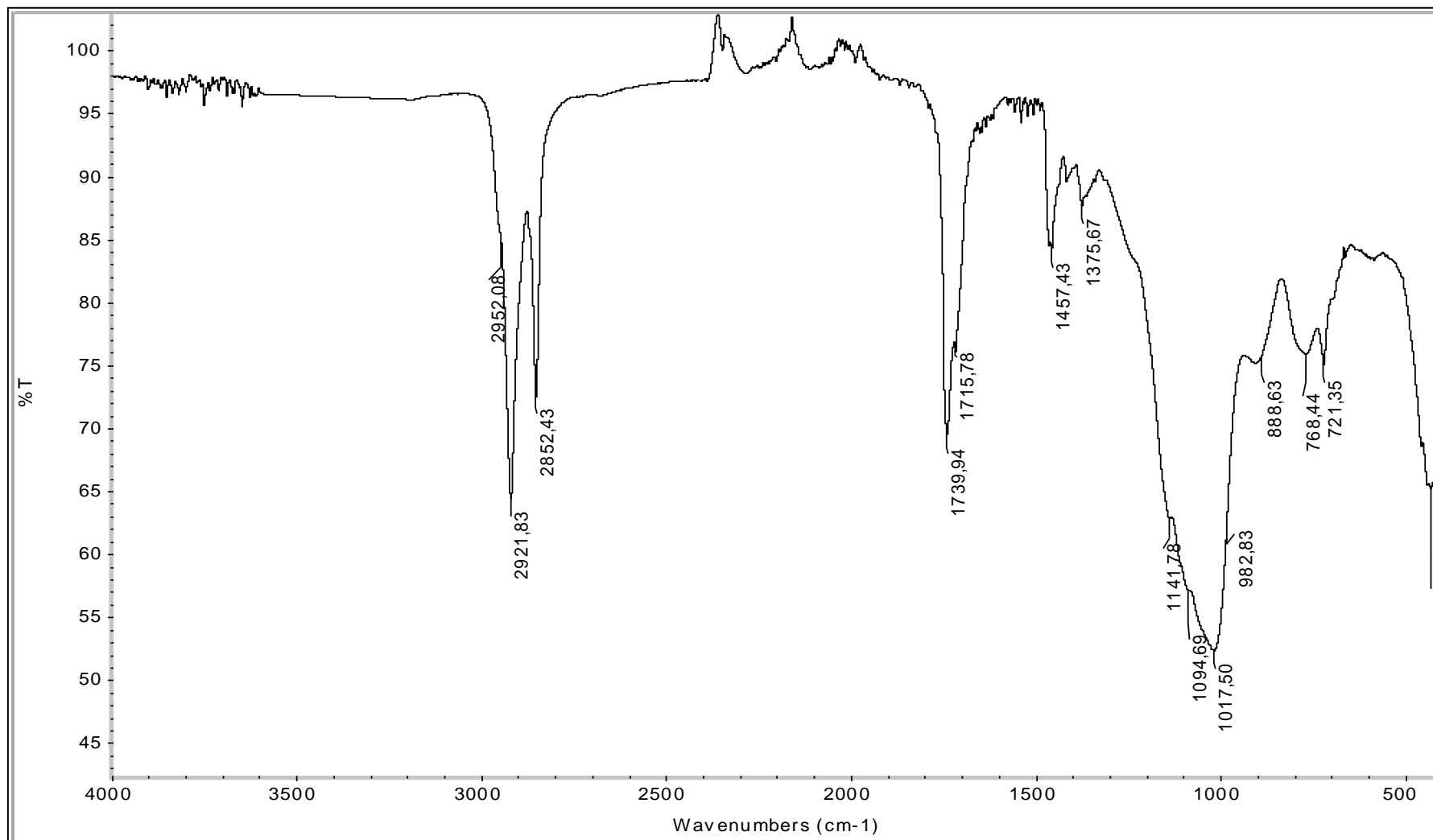


Figure 4.13. FTIR spectrum of DCM extracted VTMS γ HPS sample.

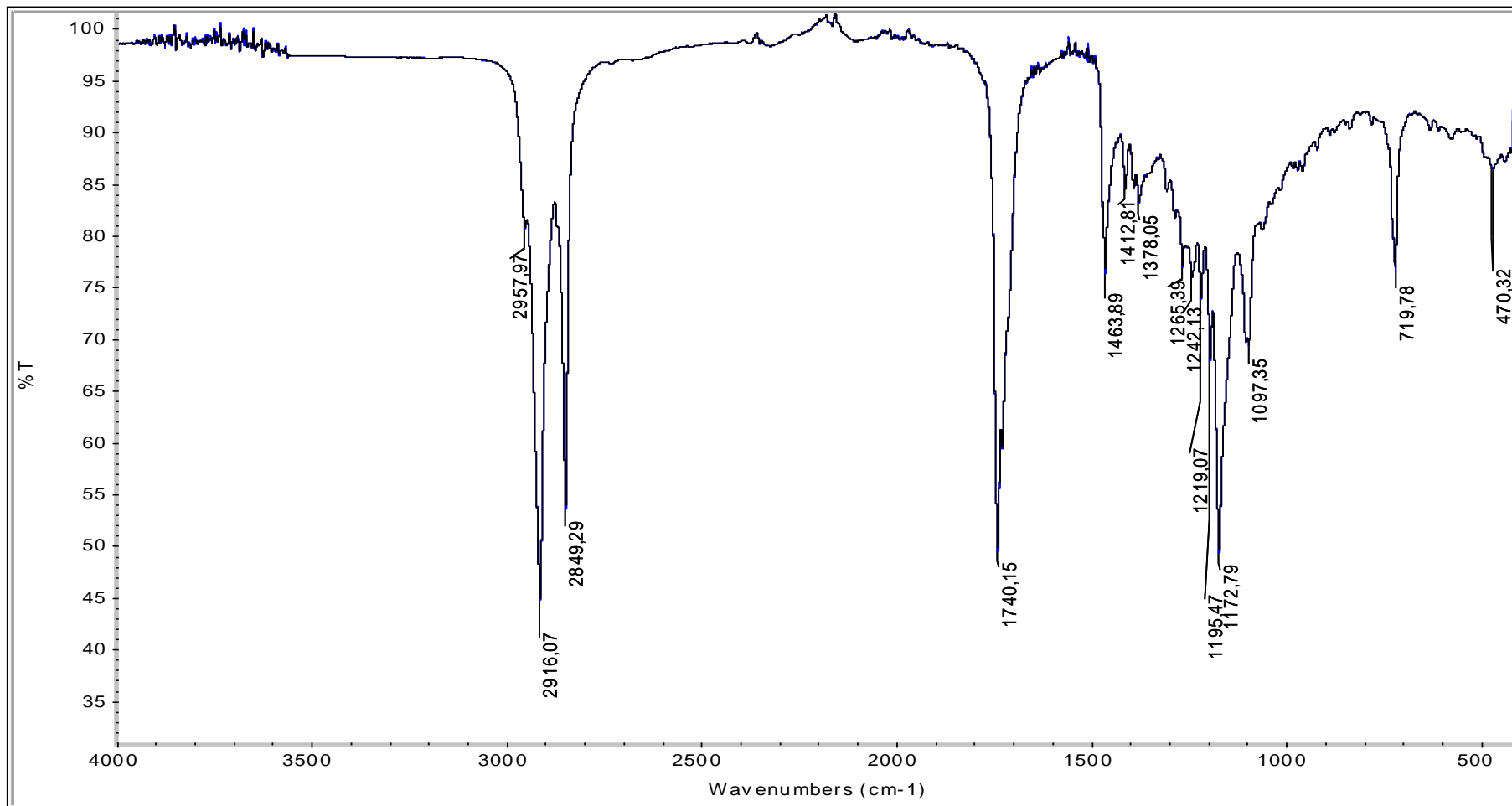


Figure 4.14. FTIR spectrum of extract of VTMS γ HPS sample.

4.4. Thermal Properties

Differential Scanning Calorimetry (DSC) technique was used to analyze the effect of moisture curing on the polymer samples. Differential Scanning Calorimetry (DSC) measures the temperatures and heat flow associated with transitions in materials as a function of time and temperature. The technique provides information about physical transformations such as phase transitions (melting, glass transition, decomposition etc.). These transitions involve endothermic or exothermic processes.

With the differential scanning method T_g values of the polymers were analyzed. Temperature scans were run from $-60\text{ }^\circ\text{C}$ to $160\text{ }^\circ\text{C}$ at a heating rate of $10\text{ }^\circ\text{C}/\text{min}$. For each sample two runs were done. On the other hand, in the second runs no T_g values were observed. Possible explanation for this situation can be further silanol condensation during the first run of analysis. This incomplete condensation continues during DSC measurements above $100\text{ }^\circ\text{C}$ and the transitions might be the endotherms caused by silanol condensation rather than T_g .

In measurements, the samples show no glass transition in the temperature range used. Figure 4.15 shows the result obtained for the silanized-HPS homopolymer for 2 different samples after moisture cure. Samples have the mol ratio of VTMS to HPS, 5:1 and 3:1. And for comparison pure raw material HPS and homopolymer of VTMS were analyzed. The melting endotherms seen in the plot are due to unreacted HPS. Small melting point depression can be explained by the lower melting point of the unreacted VTMS homopolymer which cannot be completely separated from the silanized-HPS polymer.

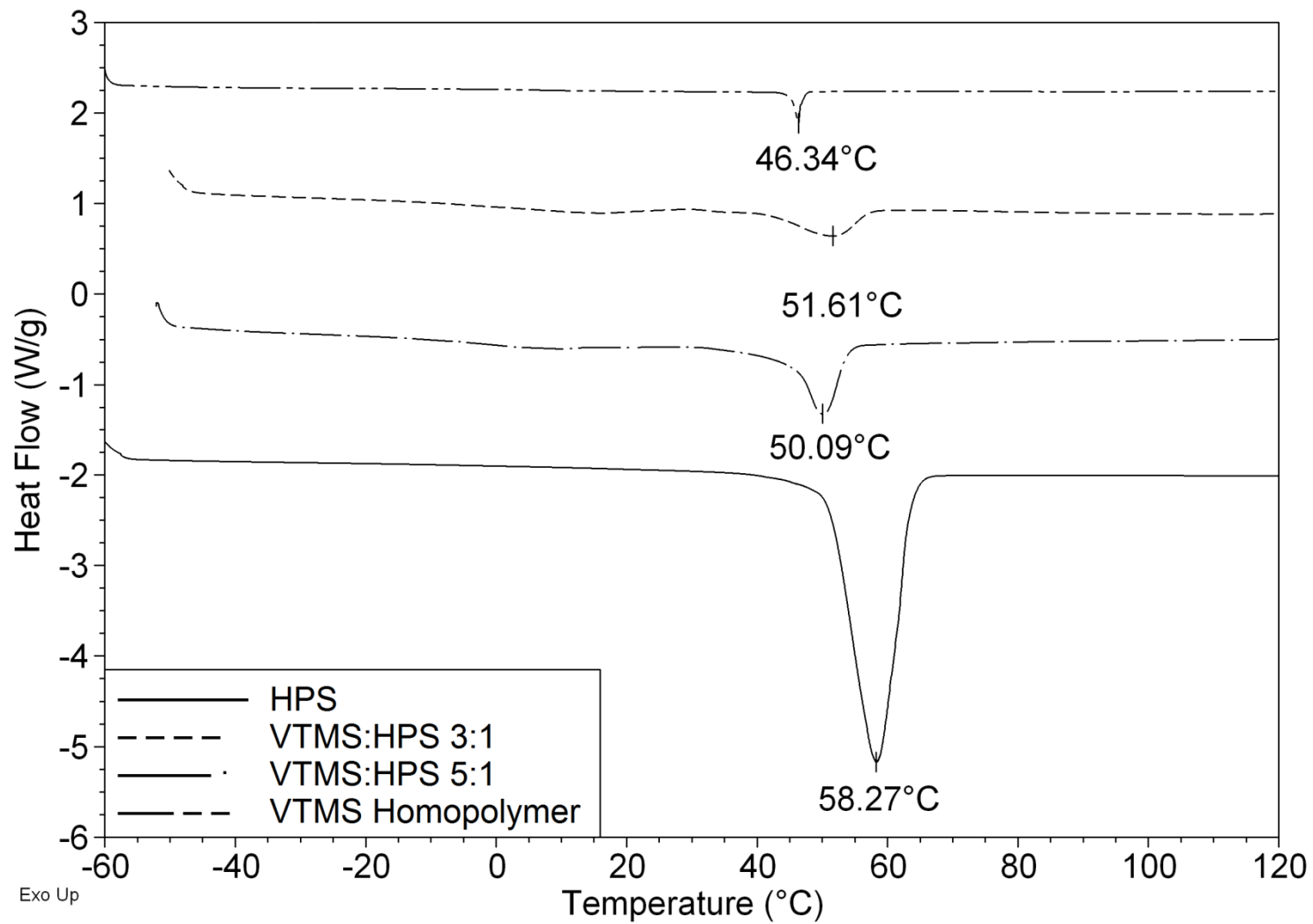


Figure 4.15. DSC traces of silanized-HPS 5:1 and 3:1 after moisture cure.

4.5. Swelling Test

Swelling occurs when the crosslinked polymers absorb the solvent that they are placed in. As the network is swollen, there is a competition between two forces. Solvent penetrates into the polymer. In return to this force, the polymer chains in the crosslinked polymer try to elongate and generate a force in opposite to deformation. The volumetric swelling ceases when two forces balance each other.

One of the methods is used to compare the relative crosslink density is swelling behavior. A highly crosslinked sample will absorb less solvent and the less crosslinked sample will absorb more solvent. With the help of this property, by measuring the change in dimensions during swelling it is possible to compare the relative crosslink density of different samples. Mostly, high crosslink density leads to small equilibrium swelling ratio.

The swelling behavior of the poly-VTMS γ HPS in CH_2Cl_2 was examined by using a traveling microscope. The samples were put in a closed container and the experiment was continued until the solvent uptake ceased. The swelling ratio (q) was obtained by the following equation:

$$q = V / V_0 = (L / L_0)^3$$

where V_0 and V are the volumes of unswollen and swollen polymer samples, respectively; and L_0 and L are the unswollen and swollen lengths of polymer samples, respectively. Swelling ratio depends upon the molar volume of the solvent, the crosslink density and crosslink segment length of the polymer. The swelling behaviors of the samples after moisture cure are shown in Figure 4.16. The polymer with high concentration of VTMS crosslinking agent swelled less after moisture cure due to high crosslink density as shown in Figure 4.16. A problem occurred during the determination of swelling behavior. In some cases, samples fragmented into small pieces when solvent penetrates into the polymer. This shows that crosslinking is not uniformly distributed in the sample. The regions having low crosslink density can be broken by solvent. This situation is called grain phenomena in literature. As the parts were made in an open mold, water removal is easier at the surface

than in the bulk of the polymer and condensation equilibrium position is effected by the efficiency of water removal.

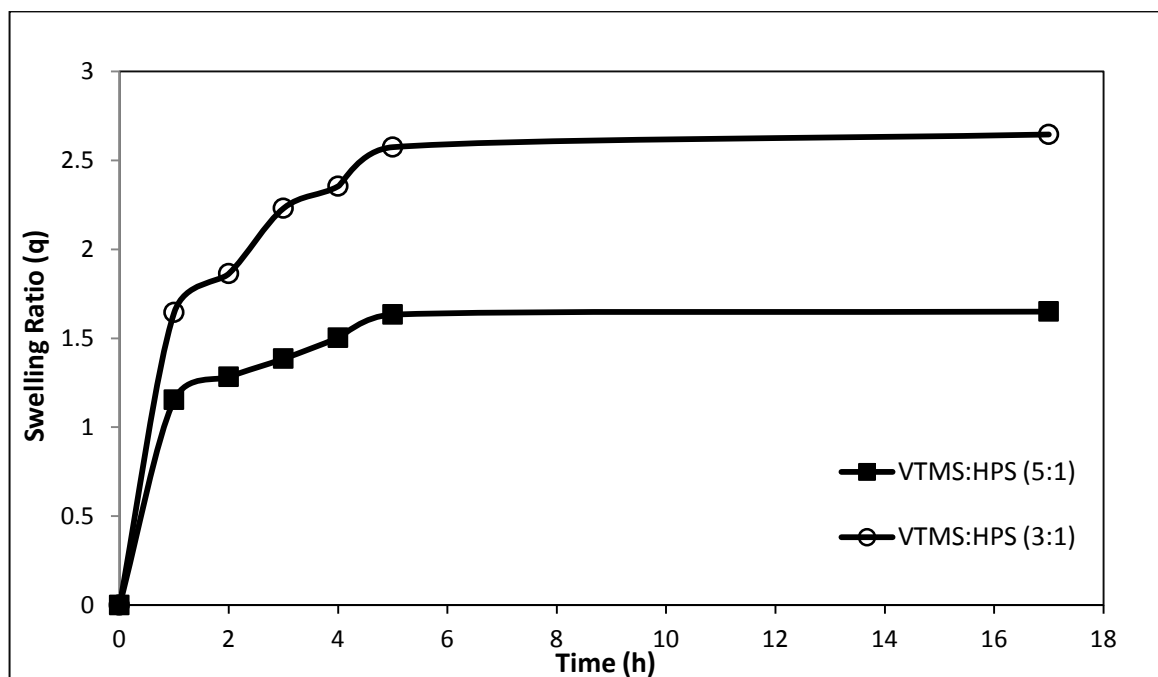


Figure 4.16. Swelling behavior of silanized-HPS with different mol ratio after moisture cure.

4.6. Adhesion and Homopolymerization of VTMS graft HPS on Glass Surface

Silanol groups liberated after hydrolysis are capable of reacting with hydroxyl containing inorganic surfaces such as glass. When VTMS graft HPS was coated on clean glass, allowed to remain in humid air and then heated to 125 °C for 48 hours gave an excellent coating on the glass surface. Figure 4.17 shows the general mechanism of the moisture curing process. After extraction with diethylether this surface was hard, insoluble and showed excellent adhesion to glass. Thus glass surface was coated with a saturated triglyceride with excellent fastness. The coating was examined in terms of contact angle and surface hardness.

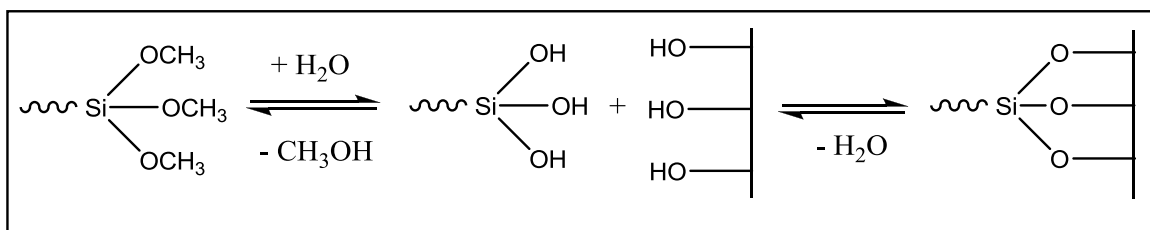


Figure 4.17. Moisture curing process of organo functional alkoxy silanes.

4.7. Contact Angle Measurements

Intermolecular interactions between liquid and solid surface provide continuous contact. This is called wetting ability of liquids. Two opposite forces play an important role in characterization of wetting. While cohesive force prevents spreading of liquid on the solid surface, adhesive force behaves in the opposite way. Contact angle measurement gives information about wettability of liquid. Three phases have to be taken in consideration during a liquid droplet is on a solid phase. Solid substrate, liquid itself and surrounding air form their own surface tensions. Young's equation explains this mechanical balance.

$$\cos\theta = (\gamma_{SV} - \gamma_{SL}) / \gamma_{LV}$$

Figure 4.18 shows where θ is the contact angle of liquid with solid surface. The surface tensions at the interphase are illustrated with solid vapor (γ_{SV}), solid liquid (γ_{SL}) and liquid vapor (γ_{LV}).

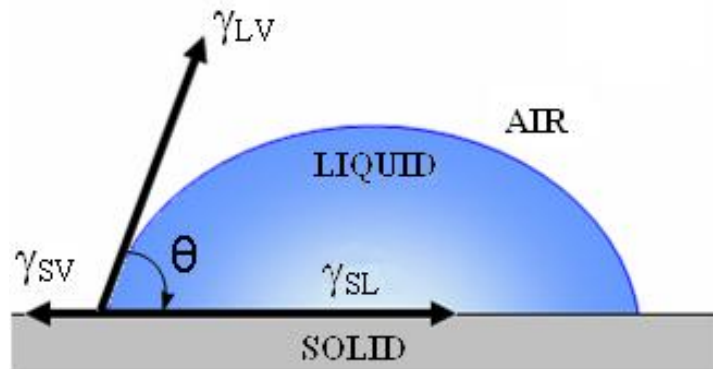


Figure 4.18. Surface tension vectors on a liquid droplet placed on a solid surface [13].

Contact angle higher than 90° indicates that wetting of the surface is unfavorable. On the other hand, contact angle less than 90° shows that wetting of the surface is very favorable. Using water during contact angle measurements gives information about the solid surface such as hydrophilicity (wettable surface), hydrophobicity (non-wettable surface), polarity and homogeneity.

Table 4.1. The relationship between contact angle, degree of wetting and strength of interactions.

Contact angle	Degree of wetting	Strength of:	
		Solid/liquid interactions	Liquid/liquid interactions
$\theta=0$	Perfect wetting	Strong	Weak
$0<\theta<90^\circ$	High wettability	Strong	Strong
		Weak	Weak
$90\leq\theta<180^\circ$	Low wettability	Weak	Strong
$\theta=180^\circ$	Perfectly non-wetting	Weak	Strong

Water contact angle measurements were done on clean glass, vinyltrimethoxysilane coated and polymerized glass and VTMS γ HPS coated and polymerized glass. The variations of contact angles give the information to compare the effect of bond between

alkoxy silane and glass surface. 10 measurements were taken from different points on the solid surface and average values are noted as results given in Figure 4.19.

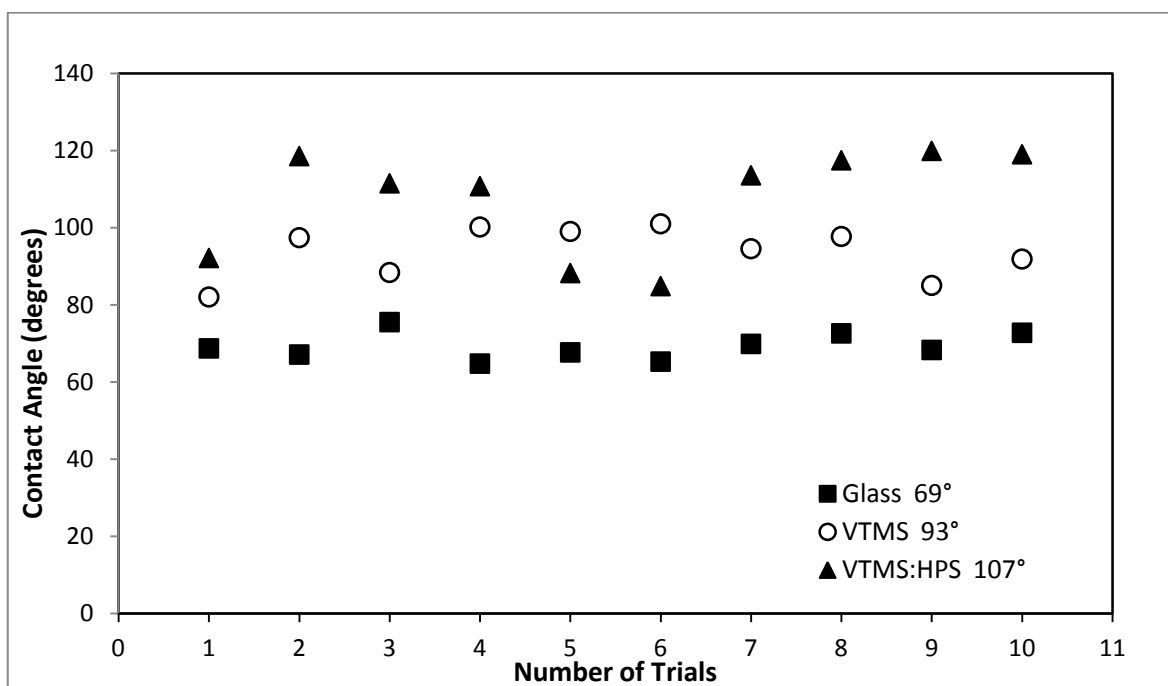


Figure 4.19. The contact angle measurements of clean glass, silanized glass and VTMS-g-HPS solution casted glass.

First of all, contact angle is measured on clean glass for comparison then VTMS is coated on glass and enough time is given for hydrolysis of alkoxy groups. Glass is heated to 125 °C to complete condensation of hydrolysis product. Contact angle is increased from $\theta=69^\circ$ to $\theta=93^\circ$. While VTMS polymerizes through silanol condensation its vinyl groups are still intact. Free vinyl groups of silane provide some hydrophobicity to glass surface. IR spectrum of VTMS coated glass is given in Figure 4.20. When VTMS is grafted on HPS, free alkoxy end groups of silane form siloxane bonds with glass surface. Long alkyl chains of triglyceride provide more hydrophobicity and increase water contact angle to $\theta=107^\circ$. In many applications of inorganic filled or glass fiber reinforced polymers it is desirable to have a hydrophobic/oleophilic surface on the filler or the fiber. VTMS γ HPS provides a cheap material for filler treatment for this purpose.

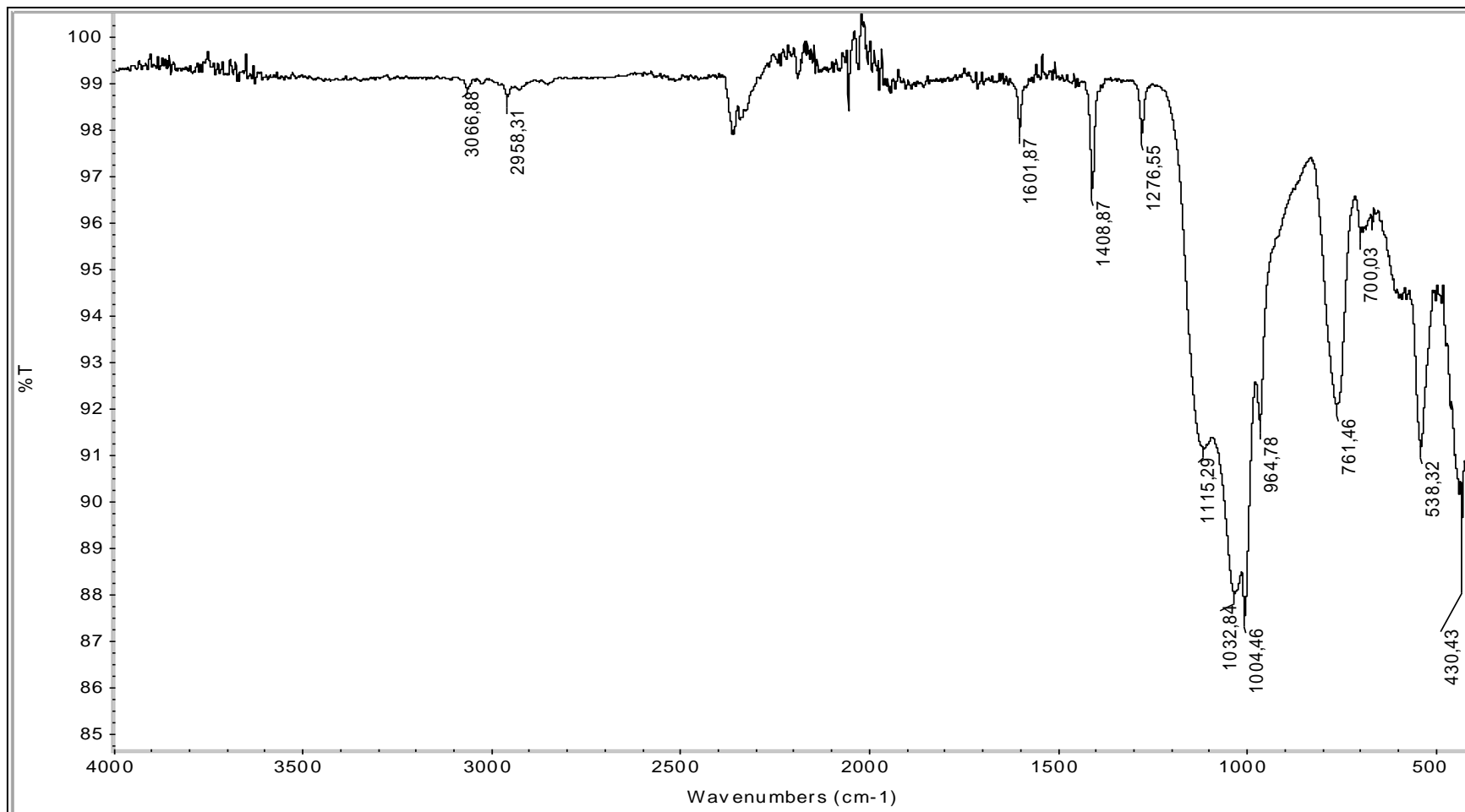


Figure 4.20. FT-IR spectrum of VTMS coated glass surface.

4.8. Surface Hardness Test

Surface hardness of the polymers was measured with Zwick/Roell Durometer according to ASTM D 2240 standard test.

The shore durometer is composed of a hardened indenter, an accurately calibrated spring, a depth indicator and a flat presser foot. Scale of the measurement of hardness is 0 for full penetration and if there is no penetration 100. The hardened indenter is placed in the middle of the pressor foot and has penetration length of 2.5 mm.

The shore type instrument works with basic principle, the 2.5 mm extended indenter is pushed by spring into the sample and the depth of the penetration is indicated by the detector scale (0-100). As the material is softer, the indentation becomes deeper. The obtained data from indicator reading is lower. If the material is harder, the obtained number is higher. For the shore test analysis polymer samples whose thicknesses 1 mm were prepared. The samples were protected from any possible mechanical stress before testing. In order to calculate an average value, the samples were tested from 10 different points on the same surface. The results for the surface hardness of the pure hydrogenated palm stearin and homopolymerized VTMS grafted HPS are given in Figure 4.21.

The results explain that as VTMS ratio increases, the improvement in the surface hardness is obtained. As VTMS ratio increases, crosslink density also increases. The results also show that polymer surface might have fluctuations on the hardness after moisture curing process. Unevenly distributed hydroxysilane groups on HPS might cause disordered crosslink density after condensation upon moisture cure. Water removal efficiency also changes inside the sample, as mentioned before. This is the reason some part of the polymer is harder than other soft segments in polymer network. As mentioned in swelling test, this result is also another consequence of the grainy morphology.

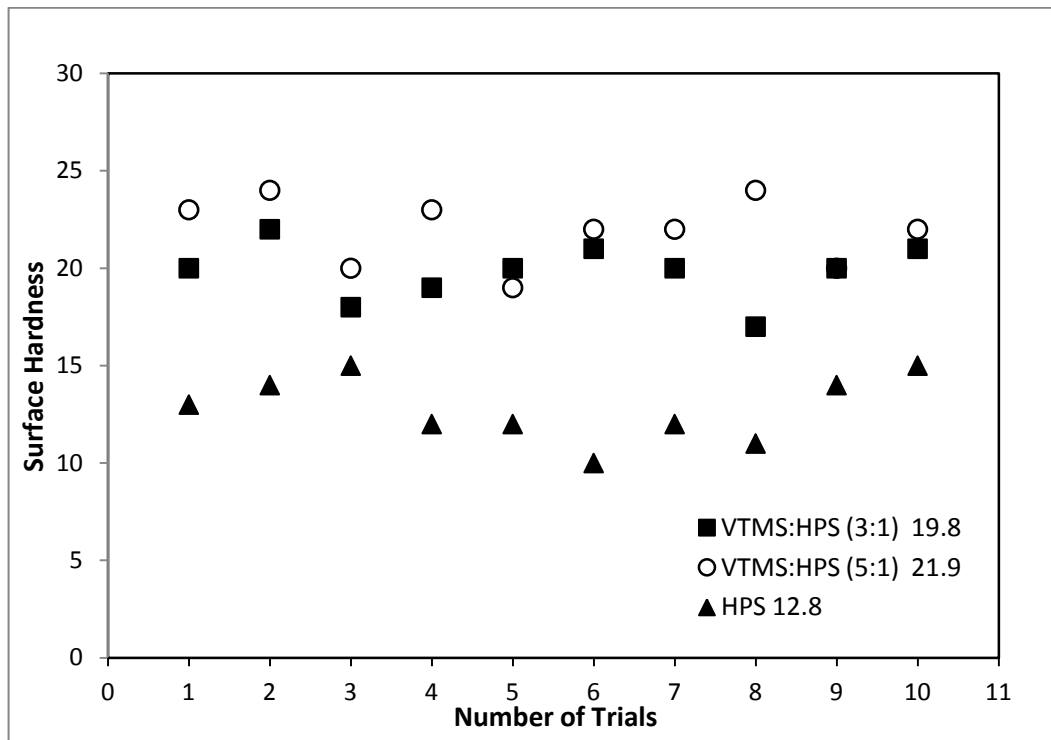


Figure 4.21. Shore test results for HPS and silanized HPS.

5. CONCLUSIONS

Saturated triglyceride was modified by the grafting reaction of vinyltrimethoxysilane in the presence of dicumylperoxide free radical initiator. The characterization of silanized-HPS was done by ^1H NMR and FT-IR spectroscopy. The average of 0.82 methyl silane functional groups per triglyceride were grafted. Methoxy groups of VTMS grafted HPS were very sensitive to moisture. In order to prevent any possible hydrolysis, silanized-HPS was used without any purification for further synthesis.

The silanized-HPS was both homopolymerized and grafted on inorganic glass surface by hydrolysis of methoxy groups followed by silanol condensation. The hydrophobicity of glass surfaces of vinyltrimethoxysilane coated and silanized-HPS coated glass was studied by water contact angle measurements. Water contact angle was $\theta=93^\circ$ and $\theta=107^\circ$, respectively. Surface properties of the silanized-HPS homopolymer were studied on glass surface by surface hardness test. Unevenly distributed hydroxysilane on HPS caused fluctuations on the hardness after moisture cure. The homopolymer of VTMS γ HPS has very poor mechanical properties due to the low crosslink density. The samples cannot be removed from the mold without fractures. Unfortunately, no mechanical test could be applied on samples by using DMA except surface hardness test. The T_g of homopolymer could not be determined by DSC. Due to low crosslink density some samples were fragmented during swelling test. The effect of increasing crosslink density was observed in the swelling test.

As a future project, the effect of the pressurized reactor equipment for the grafting reaction can be analyzed and the reactivity of different vinylsilanes can be compared.

REFERENCES

1. Baumann, H., M. Bühler, H. Fochem, F. Hirsinger, H. Zobelein and J. Falbe, "Natural Fats and Oils—Renewable Raw Materials for the Chemical Industry", *Angewandte Chemie International Edition in English*, Vol. 27, No. 1, pp. 41-62, 1988.
2. Carlsson, A. S., "Plant Oils as Feedstock Alternatives to Petroleum – a Short Survey of Potential Oil Crop Platforms", *Biochimie*, Vol. 91, No. 6, pp. 665-670, 2009.
3. Tsujimoto, T., H. Uyama and S. Kobayashi, "Synthesis of High-Performance Green Nanocomposites from Renewable Natural Oils", *Polymer Degradation and Stability*, Vol. 95, No. 8, pp. 1399-1405, 2010.
4. Narayan, R., D. Graiver, K. Farminer and M. Srinivasan, "Moisture-Curable Oil and Fat Compositions and Processes for Preparing the Same", WO Patent WO/2010/042,175 US Patent 2010.
5. Montero de Espinosa, L. and M. A. R. Meier, "Plant Oils: The Perfect Renewable Resource for Polymer Science?!", *European Polymer Journal*, Vol. 47, No. 5, pp. 837-852, 2011.
6. Seniha Güner, F., Y. Yağcı and A. Tuncer Erciyes, "Polymers from Triglyceride Oils", *Progress in Polymer Science*, Vol. 31, No. 7, pp. 633-670, 2006.
7. Öztürk, C., "Polymerization Reactions of Functionalized Vegetable Oils with Petroleum-Based Macromonomer", Ph.D. Thesis, Boğaziçi University, 2010.
8. Çolak, S., "Synthesis and Interfacial Properties of Organosilane Derivative of Acrylated Soybean Oil", M.S. Thesis, Boğaziçi University, 2006.

9. Khot, S. N., "Synthesis and Application of Triglyceride Based Polymers", Ph.D. Thesis, University of Delaware, 2001.
10. Gunstone, F. D., *Fatty Acid and Lipid Chemistry*, Blackie Acad. & Professional, London [u.a.], 1996.
11. Markley, K., S., "Fatty Acids : Their Chemistry and Physical Properties", Interscience Publishers, 1947.
12. Mutlu, H., "Polymerization of Plant Oils with P-Dinitrosobenzene", M.S. Thesis, Chemistry, Boğaziçi University, 2008.
13. Çavuşoğlu, J., "Surface Modification of Polyvinyl Alcohol Films by Functionalized Soybean Oil Triglycerides", M.S. Thesis, Boğaziçi University, 2009.
14. Friedman, A., S. B. Polovsky, J. P. Pavlichko and L. S. Moral, "Hydroxylated Milk Glycerides", US Patent 5,576,027, 1996.
15. Bussell, G. W., "Maleinized Fatty Acid Esters of 9-Oxatetracyclo-4.4.1oundecan-4-OI", US Patent 3,855,163, 1974.
16. Force, C. G. and F. S. Starr, "Vegetable Oil Adducts as Emollients in Skin and Hair Care Products", US Patent 4,740,367, 1988.
17. Eren, T. and S. H. Küsefoğlu, "Synthesis and Polymerization of the Bromoacrylated Plant Oil Triglycerides to Rigid, Flame-Retardant Polymers", *Journal of Applied Polymer Science*, Vol. 91, No. 4, pp. 2700-2710, 2004.
18. Cain, F. W., A. J. Kuin, A. C. Peilow and P. T. Quinlan, "Fat Blends Containing Diglycerides", US Patent 5,912,042, 1999.

19. Behr, A., A. Westfechtel and J. Pérez Gomes, "Catalytic Processes for the Technical Use of Natural Fats and Oils", *Chemical engineering & technology*, Vol. 31, No. 5, pp. 700-714, 2008.
20. Thomas, A., "Fats and Fatty Oils", *Ullmann's Encyclopedia of Industrial Chemistry*, 2007.
21. Ockerman, H. W. and L. Basu, "Edible Rendering--Rendered Products for Human Use", *Essential Rendering*, pp. 95-110, 2006.
22. Hill, K., "Fats and Oils as Oleochemical Raw Materials", *Pure and applied chemistry*, Vol. 72, No. 7, pp. 1255-1264, 2000.
23. Karabulut, I., M. Kayahan and S. Yaprak, "Determination of Changes in Some Physical and Chemical Properties of Soybean Oil During Hydrogenation", *Food chemistry*, Vol. 81, No. 3, pp. 453-456, 2003.
24. Singh, P., S., Trujillo, W., A., "Apparatus and Method for Defatting Meat and Products Derived Therefrom", WO/1995/023,028 US Patent (1995).
25. Langer, H. R., "Process for Reducing the Fat Content of Meats", US Patent 3,780,191, 1973.
26. Small, D. M., "Method for Making Meat Products Having a Reduced Saturated Fat and Cholesterol Content", US Patent 4,980,185, 1990.
27. King, J. W., J. H. Johnson and J. P. Friedrich, "Extraction of Fat Tissue from Meat Products with Supercritical Carbon Dioxide", *Journal of Agricultural and Food Chemistry*, Vol. 37, No. 4, pp. 951-954, 1989.
28. Singh, P. S. and W. A. Trujillo, "Method for Defatting Meat and Defatted Products", US Patent 5,944,597, 1999.

29. Singh, P. S. and W. A. Trujillo, "Method for Defatting Meat", US Patent 5,552,173, 1996.
30. Alberts, T. W., "Alberts Meat Processing", US Patent 3,177,080, 1965.
31. Poplack, W. J., "Method for Treating Beef Suet To", US Patent 3,764,713, 1973.
32. *Oils and Shortenings 101*, 2012, <http://www.cargillfoods.com/na/en/products/oils-shortenings/oils-for-healthy-solutions/overview/oils-and-shortening-101/index.jsp>, accessed at August 2012.
33. Gabrovska, M., J. Krstić, R. Edreva-Kardjieva, M. Stanković and D. Jovanović, "The Influence of the Support on the Properties of Nickel Catalysts for Edible Oil Hydrogenation", *Applied Catalysis A: General*, Vol. 299, No. pp. 73-83, 2006.
34. Fernández, M. B., G. M. Tonetto, G. H. Crapiste and D. E. Damiani, "Revisiting the Hydrogenation of Sunflower Oil over a Ni Catalyst", *Journal of food engineering*, Vol. 82, No. 2, pp. 199-208, 2007.
35. *Gelest Silane Coupling Agents : Connecting across Boundaries*, 2012, <http://www.gelest.com/goods/pdf/couplingagents.pdf>, accessed at August 2012.
36. *Silquest Silanes Product and Potential Applications*, 2012, http://www.momentiveperformancematerials.biz/momentiveInternetDoc/MPM/Static%20Files/Documents/Data%20Sheets/Silquest_Silanes_SG.indd.pdf, accessed at August 2012.
37. Kinloch, A. J., *Adhesion and Adhesives: Science and Technology*, Springer, 1987.
38. *Silanes in Filled Plastic Compounds*, 2012, <http://plastics.evonik.com/sites/dc/Downloadcenter/Evonik/Product/Plastics/en/silane-crosslinking-of-polyethylene.pdf>, accessed at August 2012.

39. Witucki, G. L., "A Silane Primer: Chemistry and Applications of Alkoxy Silanes", *Journal of coatings technology*, Vol. 65, No. pp. 57-57, 1993.
40. Arkles, B., "Tailoring Surfaces with Silanes", *Chemtech*, Vol. 7, No. 12, pp. 766-778, 1977.
41. *Selection Guide Famasil Silane Coupling Agents*, 2012, http://famastechnology.com/pdf/Famasil_Coupling_Agents.pdf, accessed at August 2012.
42. Kutz, M., *Applied Plastics Engineering Handbook: Processing and Materials*, William Andrew, pp. 503, 2011.
43. Shah, G. B., M. Fuzail and J. Anwar, "Aspects of the Crosslinking of Polyethylene with Vinyl Silane", *Journal of Applied Polymer Science*, Vol. 92, No. 6, pp. 3796-3803, 2004.
44. Murakami, K., H. Yorimitsu and K. Oshima, "Zinc-Catalyzed Nucleophilic Substitution Reaction of Chlorosilanes with Organomagnesium Reagents", *The Journal of Organic Chemistry*, Vol. 74, No. 3, pp. 1415-1417, 2008.
45. Fabris, F. W., F. C. Stedile, R. S. Mauler and S. Nachtigall, "Free Radical Modification of Ldpe with Vinyltriethoxysilane", *European Polymer Journal*, Vol. 40, No. 6, pp. 1119-1126, 2004.
46. Scott, H. G., "Cross-Linking of a Polyolefin with a Silane", US Patent 3,646,155, 1972.
47. Shieh, Y. T. and C. M. Liu, "Silane Grafting Reactions of Ldpe, Hdpe, and Lldpe", *Journal of Applied Polymer Science*, Vol. 74, No. 14, pp. 3404-3411, 1999.

48. Shieh, Y. T. and T. H. Tsai, "Silane Grafting Reactions of Low-Density Polyethylene", *Journal of Applied Polymer Science*, Vol. 69, No. 2, pp. 255-261, 1998.
49. Shieh, Y. T., H. C. Chuang and C. M. Liu, "Water Crosslinking Reactions of Silane-Grafted Polyolefin Blends", *Journal of Applied Polymer Science*, Vol. 81, No. 7, pp. 1799-1807, 2001.
50. Wu, T. S., "Infusion Method for Crosslinking Cables", *Wire & Cable Technology International*, Vol. 35, No. 1, pp. 48-50, 2007.
51. Palmlöf, M., T. Hjertberg and B. Å. Sultan, "Crosslinking Reactions of Ethylene Vinyl Silane Copolymers at Processing Temperatures", *Journal of Applied Polymer Science*, Vol. 42, No. 5, pp. 1193-1203, 1991.
52. Sirisinha, K. and S. Chimdist, "Comparison of Techniques for Determining Crosslinking in Silane-Water Crosslinked Materials", *Polymer testing*, Vol. 25, No. 4, pp. 518-526, 2006.
53. Narkis, M., A. Tzur, A. Vaxman and H. Fritz, "Some Properties of Silane-Grafted Moisture-Crosslinked Polyethylene", *Polymer Engineering & Science*, Vol. 25, No. 13, pp. 857-862, 1985.
54. Forsyth, J., W. Baker, K. Russell and R. A. Whitney, "Peroxide-Initiated Vinylsilane Grafting: Structural Studies on a Hydrocarbon Substrate", *Journal of Polymer Science Part A: Polymer Chemistry*, Vol. 35, No. 16, pp. 3517-3525, 1997.
55. Parent, J. S., R. Parodi and W. Wu, "Radical Mediated Graft Modification of Polyolefins: Vinyltriethoxysilane Addition Dynamics and Yields", *Polymer Engineering & Science*, Vol. 46, No. 12, pp. 1754-1761, 2006.
56. Huttenhower, H. A., "A Study of Silane Grafting to Model Polyethylene Compounds", PhD. Thesis, Georgia Institute of Technology, 2010.

57. *Organic Peroxides Product Guide*, 2012, http://www.pergan.com/Downloads/Pe_Products_NA.pdf, accessed at August 2012.
58. Tran, P. T., "Engineered Soy Oils for New Value Added Applications", *PhD. Thesis*, Chemical Engineering and Material Science, Michigan State University, 2005.
59. Spencer, M., J. S. Parent and R. A. Whitney, "Composition Distribution in Poly (Ethylene-g-Vinyltrimethoxysilane)", *Polymer*, Vol. 44, No. 7, pp. 2015-2023, 2003.
60. *Peroxan Dc*, 2012, <http://uzkimya.com/doc/PEROXAN%20DC.pdf>, accessed at August, 2012.